

Segmented Operations using Matrix Multiplications

Aleksandros Sobczyk

aleksandros.sobczyk@h-partners.com

Giuseppe Sorrentino

giuseppe.sorrentino@huawei.com

Anastasios Zouzias

anastasios.zouzias@huawei.com

Computing Systems Lab

Huawei Zurich Research Center

Abstract

Specialized computational units that perform small matrix multiplications as primitive operations are typically present in modern accelerators. However, these units are often underutilized for many fundamental operations besides dense matrix multiplications. The analysis of algorithms for such architectures is currently stagnated due to the lack of a rigorous theoretical model of computation that captures their characteristics. In this work, we propose *MMV-RAM*, a computational model tailored to matrix multiplication accelerators. *MMV-RAM* judiciously extends the *Vector-RAM* model with an additional processing unit that multiplies two matrices of sizes $n \times s$ and $s \times s$ in a single parallel step, where s is a model parameter. We provide a detailed theoretical analysis of the model, and carefully balance the computational power between the matrix and vector units, guided by the circuit complexity lower bound that parity is not in $AC[0]$.

In *MMV-RAM*, we study algorithms for *segmented scan and sum*, two fundamental parallel primitives. We propose a segmented scan algorithm that uses matrix multiplications to perform *speculative* block-scan computations, which runs in $\mathcal{O}(\log_s(n))$ steps. In contrast, we show that any algorithm that uses only the vector unit of *MMV-RAM* requires $\Omega\left(\frac{\log_2(n)}{\log_2 \log_2(n)}\right)$ steps. We further apply these techniques to obtain similar theoretical speedups for element-wise vector multiplication and matrix multiplication. Beyond the worst-case complexity analysis, we propose algorithms for segmented operations that could lead to highly efficient and pragmatic implementations. For example, we observe that segmented sum is a combination of three elementary parallel primitives: scan, compress, and vector differentiation. As a case study, we implement and experimentally evaluate the proposed algorithms using the Ascend AI 910B accelerator, which contains both matrix multiplication and vector cores, demonstrating significant speedups against a vector-only baseline.

1 Introduction

In recent years, the unexpectedly rapid evolution and development of Artificial Intelligence (AI) and, in particular, deep learning have strongly influenced the computing industry. Deep learning workloads, both training and inference, demand more and more performance every year [31]. The high demand for accelerated AI computing has resulted in manufacturing domain-specific accelerators that contain, most notably, specialized Matrix Multiplication Unit (MMU). Examples of such accelerators and MMU that have been massively produced include NVIDIA Tensor Cores [43], Google TPU Matrix Multiplication unit [30], and Huawei Ascend’s Cube unit [35], to name a few. These MMU have helped to increase the peak arithmetic performance for regular and dense computations.

Although MMU have proven highly effective for regular and dense computations, such as convolutions, the attention mechanism in transformer architectures [56], and fully connected layers in deep learning, their applicability to irregular and sparse computations remains uncertain. In particular, sparsity in deep learning is a well-known characteristic that has not yet been successfully exploited in practice [25, 18, 13]. Therefore, there is a debate in the computing industry on whether specialized computing units for sparse computations, usually referred to as “Sparse Tensor Cores”, should be designed [58, 42, 24], or if irregular and sparse computations should be handled using the already existing MMUs along with algorithmic innovations [14, 15, 63, 44, 33]. In this work, we follow the latter approach of developing algorithmic innovations using MMU as initiated in [15] and revisit segmented operations (scan and sum) in this new setting. The motivation why we focus on segmented operations is that, first, they are

fundamental computational paradigms in parallel computing with various applications [6, 49, 12]; second, the most prominent application of segmented sums is irregular sparse matrix-vector multiplication [9, 37] which is of great importance to efficiently address irregular and sparse computations in the near future.

The analysis of parallel algorithms, especially for prefix sum or scan problems, is well-established in parallel models of computation such as the Parallel RAM (PRAM) [50, 28, 20], Bulk Synchronous Parallel (BSP) [55, 39, 40, 54], LogP [16], Vector-RAM [46, 7], the TCU Model (the first that tries to model matrix multiplication accelerators) [14, 15], and circuit models [20, 57, 59, 34]. As we target AI Accelerators, containing both matrix and vector units, the two most relevant models are arguably TCU and Vector-RAM, but none of them fully embrace the accelerator heterogeneity, as we discuss next.

The TCU model is not suitable for our purposes because it omits any form of vector processing unit. This omission is both technically non-trivial to address (as we discuss extensively in this work), and essential for accurately modeling modern architectures. Indeed, Vector Unit (VCU) are typically present near the matrix multiplication units in AI accelerators, since element-wise activation operations are ubiquitous in AI workloads. For example, in convolutional neural networks, convolutions are followed by the ReLU activation function [32], and, in the transformer architecture, the linear layers of FFN are followed by the specialized GELU activation function [56].

The Vector-RAM model, instead, also presents some limitations in our context. First, it does not entail an explicit representation of matrix multiplication units, making it inadequate for reasoning about algorithms that depend heavily on such operations. Moreover, its vector instruction set is overly powerful: they can perform operations like prefix sums, or even matrix multiplication, in a single step [7]. With such a powerful vector unit, an explicit matrix multiplication unit becomes obsolete.

1.1 Contributions

To address the aforementioned limitations of both the Vector-RAM and the TCU model, we propose an extension of the Vector-RAM model, called *MMV-RAM*, which includes an additional Matrix Multiplication unit, along with the Vector unit. The MMU handles matrix multiplications of sizes $n \times s$ and $s \times s$ in a single step ($s \geq 2$ is a model parameter), whereas the VCU is used for elementary vector operations.

Our key technical contribution in the design of the MMV-RAM model is the separation and balancing of computational power between the matrix and vector units, ensuring that they complement rather than subsume each other. This balance is grounded in a fundamental result from circuit complexity: the parity function cannot be computed by constant-depth, polynomial-size (denoted by AC[0]) circuits [21, 62, 22]. Therefore, as long as the vector unit of MMV-RAM is restricted to AC[0], then it cannot efficiently simulate the matrix unit, thus maintaining a clear computational distinction between the two units.

MMV-RAM adopts a standard work/depth cost framework, enabling an intuitive analysis of algorithms and overcoming the restrictive external-memory model view of the TCU model [15, Section 5]. For algorithm engineers, it is straightforward to use MMV-RAM for algorithmic analysis: the step complexity is given by the number of matrix and vector operations, while the total work is the sum of the costs of these operations.

Given the definition of the MMV-RAM model, we next design and analyze algorithms, starting with segmented operations. Algorithm 4.1 is an MMV-RAM segmented scan algorithm that executes (speculative) unsegmented scan operations using the MMU, and then efficiently corrects the mispredicted scans with the vector unit. The following theorem, which is proved in Section 4.3, summarizes its analysis.

Theorem 1.1 (Informal version of Theorem 4.4). *Given a value vector \mathbf{x} with bounded integer elements $|\mathbf{x}(i)| \leq M$, and a boolean vector \mathbf{f} , both of size n , Algorithm 4.1 computes the segmented scan \mathbf{z} of \mathbf{x} over \mathbf{f} . Assuming that in MMV-RAM a single matrix multiplication between two $n \times s$ and $s \times s$ matrices requires $O(ns^2)$ operations (work), the algorithm requires:*

- $O(\log_s(n))$ steps,
- $O(nB(s + \frac{B}{s}))$ total work,

where B is the number of bits-per-element. On the contrary, any algorithm that uses only the vector unit and executes work that scales polynomially in n requires $\Omega\left(\frac{\log(n)}{\log(\log(n))}\right)$ steps.

In summary, our main contributions are the following:

1. The MMV-RAM model of computation is proposed as an extension of the Vector-RAM model that contains both matrix multiplication and vector computing units, targeting matrix multiplication / AI accelerators. We provide a detailed analysis of the model, carefully balancing the power of the two units by exploiting the classic parity lower bound from circuit complexity.
2. In the MMV-RAM model, we design an $O(\log_s(n))$ -depth segmented scan algorithm (Algorithm 4.1) and analyze two fundamental applications, namely, element-wise vector multiplication and matrix multiplication. Our analysis indicates that by exploiting the MMU, we can achieve a provable theoretical speedup, compared to any MMV-RAM algorithm that uses only vector instructions.
3. Furthermore, we design multi-core speculative algorithms for segmented scan/sum, (Algorithms 5.1 and 5.2), as straightforward compositions of a few fundamental parallel primitives, applying speculation over the full input range. These algorithms are implemented on the Ascend 910B AI accelerator, which features matrix multiplication and vector processing cores. By leveraging speculative execution and effectively utilizing the matrix cores, we achieve substantial performance gains compared to vector-only baselines.

1.2 Notation

Matrices and vectors are denoted by capital and small letters, respectively, in bold font. We denote by \mathbf{U}_s the upper-triangular all-ones square matrix of size s (including the ones on the diagonal). All vectors are considered column vectors, and \mathbf{A}^\top and \mathbf{x}^\top denote the transpose of matrix \mathbf{A} and vector \mathbf{x} , respectively. Vectors and matrices are zero-index based. For a vector \mathbf{x} , $\mathbf{x}(i)$ is the $(i + 1)$ -th entry, and for integers $i < j$, we denote by $\mathbf{x}(i : j)$ the subvector $(\mathbf{x}(i), \mathbf{x}(i+1), \dots, \mathbf{x}(j-1))$. $\mathbf{x}(i : j : s)$ is the s -strided subvector with offset i : $(\mathbf{x}(i), \mathbf{x}(i+s), \mathbf{x}(i+2s) \dots, \mathbf{x}(j-1))$. If j is omitted, that is, when we write $\mathbf{x}(i :: s)$, then it defaults to the length of \mathbf{x} . For a vector \mathbf{x} of length n , the operation $\mathbf{z} \leftarrow \text{MATMUL}(\mathbf{x}, \mathbf{A})$ denotes that \mathbf{x} is viewed as a matrix \mathbf{X} of size $\lceil n/s \rceil \times s$, in a row-major order (zero-padded if necessary), and the result \mathbf{z} is a vector containing the elements of the matrix product $\mathbf{X}\mathbf{A}$, in row-major order as well. “Hat” accents on vectors, e.g. $\widehat{\mathbf{x}}$, denote the scanned version of the vectors. The “bar” accent typically denotes that all consecutive blocks of length s are prefix-summed within each block, e.g., $\bar{\mathbf{x}} \leftarrow \text{MATMUL}(\mathbf{x}, \mathbf{U}_s)$. All logarithms are base two, unless explicitly specified. For a matrix \mathbf{A} , $\|\mathbf{A}\|_{\max}$ is the maximum absolute value over all matrix elements.

1.3 Outline

In Section 2, we recall some basic definitions and background. In Section 3 we describe the MMV-RAM model. The main algorithms for segmented operations and their applications are described in Sections 4, 5, and 6. In Section 7, we provide an experimental evaluation of the proposed algorithms as a case study of the MMV-RAM model on Ascend accelerators. Section 8 outlines potential extensions and/or variants of the MMV-RAM model. We finally conclude in Section 9.

2 Background and definitions

In this section, we define the segmented scan and segmented sum tasks. Furthermore, we discuss a block-recursive approach to computing segmented scans. In the (unsegmented) scan task, we are given an array \mathbf{x} of length n and the task is to return an array \mathbf{z} of length n such that $\mathbf{z}(i) = \sum_{j \leq i} \mathbf{x}(j)$ for each i . The segmented scan task is a generalization of the scan task, where the input is divided into multiple segments, and the scan operation is performed independently within each segment:

Problem 2.1 (Segmented Scan). *Given two arrays \mathbf{x} and \mathbf{f} both of length n , where $\mathbf{f}(i)$ is a boolean value indicating whether $\mathbf{x}(i)$ is the first element of a segment, the segmented scan returns an array $\mathbf{z} = (\mathbf{z}(0), \mathbf{z}(1), \dots, \mathbf{z}(n-1))$ such that:*

$$\mathbf{z}(i) = \begin{cases} \mathbf{x}(i), & \text{if } i = 0 \text{ or } \mathbf{f}(i) = 1 \text{ (segment start)} \\ \mathbf{z}(i-1) + \mathbf{x}(i), & \text{otherwise.} \end{cases} \quad (1)$$

Segmented sum is defined accordingly in Problem 2.2. It is implicitly assumed that $f(0) = 1$.

Problem 2.2 (Segmented Sum). *Given the tuple (\mathbf{x}, \mathbf{f}) as in Problem 2.1, let N be the number of segments, $\{p_0 = 0, p_1, p_2, \dots, p_{N-1}\}$ be their starting indices, and $p_N = n$. The segmented sum (or reduction) of \mathbf{x} over \mathbf{f} is the array $\mathbf{z} = (z(0), z(1), \dots, z(N-1))$, where $z(i) = \mathbf{x}(p_i) + \dots + \mathbf{x}(p_{i+1} - 1)$.*

An example of a segmented scan is shown in Equation (2):

$$\mathbf{x} = (2, 2, 3, 3, 1, 3, 1, 2), \quad \mathbf{f} = (1, 0, 1, 0, 0, 1, 0, 0), \quad \mathbf{z} = (2, 4, 3, 6, 7, 3, 4, 6). \quad (2)$$

The corresponding segmented sum of this example would be $\mathbf{z} = (4, 7, 6)$.

In the literature, scan problems typically assume a binary associative operator, i.e., a semi-group structure (see, e.g., [6, 20]). The algebraic properties of the binary scan operator that are required from our algorithms for segmented operations are more restrictive due to speculative execution. In particular, we require that the set of input elements with the corresponding binary operation form a *group*, since we require an identity element and inverses to revert speculative operations.

We will also use the compaction (also known as compress) operation. Given \mathbf{x} and \mathbf{f} , compress returns all entries of \mathbf{x} whose corresponding entry on \mathbf{f} is set to true/one. For the example of Equation (2), COMPRESS(\mathbf{x}, \mathbf{f}) returns (2, 3, 3).

2.1 Model definitions: Vector-RAM, TCU, and circuits

Here, we provide some background on the models of computation that we will discuss throughout the paper.

Circuits

A circuit is a Directed Acyclic Graph (DAG) $G = (V, E)$. Nodes with zero in-degree are called *inputs*, and nodes with zero out-degree are called *outputs*. $|E|$ is the *size* of the circuit, whereas its *depth* is the longest path from an input to an output. The *fan-in* is the largest in-degree, and the *fan-out* is the largest out-degree. The vertices are also called *gates*, and they perform mathematical operations on their predecessors. In the scope of this work, the following types are considered:

- *Boolean circuits* consist of $\{\wedge, \vee, \neg\}$ gates that operate on boolean variables. The \wedge and \vee gates have unbounded fan-in by default, unless specified otherwise.
- *Threshold circuits* are boolean circuits which also include so-called *threshold* or *majority* gates, i.e., gates which receive as input k boolean variables x_1, \dots, x_k and return 1 if and only if $\sum_{i=1}^k w_i x_i \geq t$, for some fixed integers t, w_1, \dots, w_k .

For $i \in \mathbb{N}$, NC[i], AC[i], and TC[i] are the classes of boolean circuits with fan-in two, unbounded fan-in, and threshold circuits, respectively, all having $n^{O(1)}$ size and $O(\log^i(n))$ depth, where n is the input size. It is known that $\text{NC}[0] \subset \text{AC}[0] \subset \text{TC}[0] \subseteq \text{NC}[1]$ (see e.g. [57, Corollary 4.35]). We consider only so-called *uniform families of circuits*, i.e., their description does not change significantly for different input sizes [10, 57].

Vector-RAM

Following the definition of [7], the Vector-RAM model is a RAM model with a vector processor that executes operations on vectors of length n (the length can vary). Each vector element/word has bit-width $O(\log(n))$. Vector operations/instructions are typically assumed to admit circuits with $O(\log(n))$ depth and polynomial size, i.e., NC[1] circuits. Each vector operation is assumed to take constant time, or “one step”. The vector processor can read/write n consecutive words from/to the main memory, also in constant time. A strong aspect of the model is that Vector-RAM algorithms can be efficiently ported to other parallel models, such as PRAM.

TCU

The (s^2, l) -TCU model [14, 17], is a RAM model equipped with a uniform family of circuits that can multiply two matrices \mathbf{A} and \mathbf{B} with sizes $n \times s$ and $s \times s$, respectively ($n \geq s$). The computational cost (time complexity) of invoking the circuit is $O(ns + l)$, where the first term ns is accounted for loading the data from the main memory and writing the result, while l is a system-dependent parameter that corresponds to the latency of invoking the tensor core. The tensor core can read/write ns consecutive words from/to the main memory in constant time. Each word (and matrix element) consists of B bits, where $B \in O(\log(n))$.

3 MMV-RAM: a model for matrix multiplication AI accelerators

We propose the MMV-RAM model by judiciously extending the Vector-RAM model with a MMU. As illustrated in Figure 3.1, MMV-RAM contains the following three processing units:

- A scalar unit, capable of performing basic arithmetic, address calculations, and logic operations;
- A VCU, which performs a single vector operation in every step;
- An MMU, that multiplies two matrices of size $n \times s$ and $s \times s$ in a single step (similar to the TCU model, but without a delay parameter).

The positive integer s is the only parameter of the model, which corresponds to the (right) matrix multiplication size and it is independent of the input length¹. To be more precise, the MMU is a uniform family of circuits [10, 57] that is assumed to perform a single-step matrix multiplication. The VCU in MMV-RAM implements a fixed set of instructions defined by a uniform family of AC[0] circuits, i.e., boolean circuits with unbounded fan-in, constant depth, and polynomial size (a detailed analysis of these instructions is provided in Section 3.3). Table 3.1 summarizes how existing AI accelerators map on the proposed MMV-RAM model.

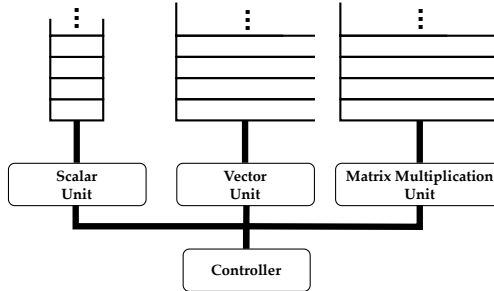


Figure 3.1: The architecture of the MMV-RAM model. MMV-RAM is based on an AC[0]-restricted Vector-RAM model [7] with the addition of a matrix memory, an MMU, and a matrix input/output port as in [14, 15].

Table 3.1: Examples of architectures where MMV-RAM can be used for algorithmic analysis.

| Architecture | Matrix Multiplication Unit | Vector-like Unit |
|-------------------|---------------------------------|------------------------------|
| NPU (AMD) [27] | Systolic array of Compute Tiles | Single compute tiles |
| NPU (Huawei) [36] | Cube Unit | Vector Unit |
| NPU (Tesla) [53] | MAC Core | SIMD Unit |
| GPU (AMD) [1] | CDNA Matrix Core (MI300 series) | SIMD Units |
| GPU (NVIDIA) [38] | Tensor Cores | Cuda Cores |
| TPU (Google) [29] | Matrix Multiply Unit (MXU) | Vector Processing Unit (VPU) |

¹Typical values of s in existing architectures are 16, 32, 128 or 256.

Table 3.2: Existing upper and lower bounds for the size of constant-depth, unbounded fan-in circuits for the product of two $s \times s$ matrices.

| Gates | Depth | Size upper bound | Size lower bound | Input | Notes |
|-------------------------------------|------------------|--|---|------------------------|--|
| $\{+, \times\}$ | $d = 2$ | $O(s^3)$ | $\Omega(s^3)$ [48] | Real numbers | Textbook algorithm |
| $\{\wedge, \vee, \neg\}$ | $d = O(1)$ | $s \exp(s)$ | $\exp(\Omega(s^{\frac{1}{d-1}}))$ [22] | $O(\log(s))$ -bit ints | See also Appendix A.1 |
| $\{\wedge, \vee, \neg, \text{Th}\}$ | $O(d), d \geq 1$ | $\tilde{O}(ds^{a+\beta\gamma^d})$ [45] | $\Omega\left(s^{\frac{2\lambda_d(s^2)}{d^2}}\right)$ [48] | $O(\log(s))$ -bit ints | $a = \log_2(7), \beta \approx 1.6, \gamma \approx 0.5$ |

3.1 Work/depth cost model

An MMV-RAM algorithm is evaluated using the *work* and *depth* analysis as in the Vector-RAM model [8, 7]. At each *step*, the machine can execute a scalar instruction, a vector instruction, or a matrix multiplication. To keep the cost model of MMV-RAM simple, we focus on bounding the number of VCU and MMU calls (i.e. *step* complexity) and their length (*element* complexity [7]).

The *work complexity* in each step represents the total number of basic (boolean) operations that are executed, potentially in parallel. In a vector instruction, for example, the work depends both on the length of the input vector and also on the number of edges (size) of the corresponding circuit that implements it. Respectively, in a matrix multiplication operation, the work depends on the number of rows of the (left) input matrix, and the bit-width of the matrix elements.

We assign the following costs for operations:

- $\mathcal{M}(n)$ is the work for matrix multiplications between two matrices with sizes $n \times s$ and $s \times s$. It scales linearly in n , which means that we can write $\mathcal{M}(an) = a\mathcal{M}(n)$ and $\mathcal{M}(n+a) = \mathcal{M}(n) + \mathcal{M}(a)$.
- $\mathcal{V}(n)$ is the work for vector instructions on vectors of length n . The only instructions that are assumed “by default” in the model are AND, OR, and NOT, which correspond to vector variants of \wedge, \vee , and \neg , respectively.

An example MMU implementation with the aforementioned properties can be achieved by a TC[0] circuit that implements the classical dot-product based matrix multiplication algorithm. The size of such a circuit is upper bounded by $\mathcal{M}(n) \in O(ns^2)$. We refer to [45] for details, and to Table 3.2 for an overview of existing upper and lower bounds. If complex vector instructions are used by an algorithm, their associated circuit sizes, depths, fan-in, and fan-out must be explicitly defined, since they affect the total work of an algorithm. In Table 3.3, for example, we describe in detail the VCU instructions that we use for our algorithms, and their corresponding costs.

Memory accesses are modeled as follows. The VCU can read n consecutive words from the main memory in one step, where n is arbitrary. The MMU can also read ns consecutive words from the main memory in a single step. These words are either stored in the $n \times s$ or in the $s \times s$ buffer of the unit. The memory layout of the input and output matrices in MMV-RAM can be any fixed matrix layout, say row or column major. Without loss of generality, we assume that the input matrices are read in row-major order, and the output matrix is also returned in row-major order. Matrix transposition of a matrix having s columns can be implemented as a dedicated vector instruction, if required. Last but not least, irregular and strided memory accesses are *not* explicitly allowed, but could be implemented with a dedicated AC[0] circuit family in the VCU. In this case, the precise circuit definition must be explicitly mentioned.

Remark 3.1. *Instructions that involve arithmetic operations can increase the number of bits required to store the (intermediate) results. For example, integer vector addition/subtraction can increase the number of bits by one, while integer multiplication can double the number of bits. For each algorithm we report upper bounds on the number of required bits to avoid overflow in the results, and the implications on the total complexity.*

3.2 The balance between the MMU and VCU

We now provide some arguments that both units of MMV-RAM are necessary to design efficient algorithms: the MMU cannot be efficiently simulated by the VCU, but the VCU provide crucial capabilities that are hard for the MMU. We first recall the foundational circuit complexity lower bound that parity is not in AC[0] [21, 62, 22].

Table 3.3: Circuit sizes and fan-in for vector operations of length n used in the main Algorithm 4.1. Integers (int) have bit-width B . All circuits have constant depth, and s is the fixed model parameter. By default, only instructions 1. and 2. are assumed by the MMV-RAM model. The remaining instructions (except REVSPEC) are also typically present in existing architectures, potentially with small variations.

| Operation | Size | Fan-in / -out | Description |
|--|----------------------------|--------------------|--|
| 1. $z : \text{vec}[\text{bit}] \leftarrow \text{AND/OR}(x : \text{vec}[\text{bit}], y : \text{vec}[\text{bit}])$ | $O(n)$ | $O(1)$ | $z(i) \leftarrow x(i) \wedge y(i)$ (resp. $x(i) \vee y(i)$). |
| 2. $z : \text{vec}[\text{bit}] \leftarrow \text{NOT}(x : \text{vec}[\text{bit}])$ | $O(n)$ | $O(1)$ | $z(i) \leftarrow \neg x(i)$. |
| 3. $z : \text{vec}[\text{int}] \leftarrow \text{MASK}(x : \text{vec}[\text{int}], y : \text{vec}[\text{bit}])$ | $O(nB)$ | $O(1) / O(B)$ | $z(i) \leftarrow x(i)$ if $y(i) = 1$, else $z(i) \leftarrow 0$. |
| 4. $z : \text{vec}[\text{bit}] \leftarrow \text{ISZERO}(x : \text{vec}[\text{int}])$ | $O(nB)$ | $O(B) / O(1)$ | $z(i) \leftarrow 1$ if $x(i) = 0$, else $z(i) \leftarrow 0$. |
| 5. $z : \text{vec}[\text{int}] \leftarrow \text{ADD/SUB}(x : \text{vec}[\text{int}], y : \text{vec}[\text{int}])$ | $O(nB^2)$ | $O(B)$ | $z(i) \leftarrow x(i) + x(j)$ (resp. $x(i) - x(j)$). |
| 6. $z : \text{vec}[\text{int}] \leftarrow \text{FILLS}(x : \text{vec}[\text{int}]; s)$ | $O(nB)$ | $O(1) / O(s)$ | $z(is : is + s) \leftarrow x(is), i \in \{0, \dots, \lfloor \frac{n}{s} \rfloor\}$. |
| 7. $z : \text{vec}[\text{int}] \leftarrow \text{GATHERS}(x : \text{vec}[\text{int}]; s)$ | $O(sB)$ | $O(1)$ | $z(i - 1) \leftarrow x(si - 1), i \in \{1, \dots, \lfloor \frac{n}{s} \rfloor\}$. |
| 8. $z : \text{vec}[\text{int}] \leftarrow \text{SCATTERS}(x : \text{vec}[\text{int}]; s)$ | $O(sB)$ | $O(1)$ | $z(si - 1) \leftarrow x(i - 1), i \in \{1, \dots, \lfloor \frac{n}{s} \rfloor\}$. |
| 9. $z : \text{vec}[\text{int}] \leftarrow \text{REVSPEC}(\bar{x} : \text{vec}[\text{int}], \bar{f} : \text{vec}[\text{int}]; s)$ | $O(nB(s^2 + \frac{B}{s}))$ | $O(s + B) / O(sB)$ | Reverts misspeculation (Lemma 4.1). |

Theorem 3.2 (Restatement of [22], Thm. 1). *For every $s > s_0^d$, where s_0 is a constant, the size L of a depth- d boolean circuit that computes the parity of s bits has size $L > 2^{(0.1) \frac{d}{d-1} s^{\frac{1}{d-1}}}$.*

Solving for d gives the following trade-off:

$$d > \frac{\log(s)}{\log(\log(L)) + c_1} + c_2, \quad (3)$$

where c_1 and c_2 are constants. This allows us to prove a clear separation between the computational power of the MMU and the VCU in the MMV-RAM model. A simple example is the following.

Fact 3.3. *Let \mathbf{A} and \mathbf{B} be two B -bit integer matrices with sizes $n \times s$ and $s \times s$, respectively. Let \mathcal{A} be an algorithm in the MMV-RAM model that uses only the scalar and the vector units to compute the matrix product \mathbf{AB} . If the work of \mathcal{A} is upper bounded by $s^{O(1)}$, then \mathcal{A} necessarily executes $\Omega(\frac{\log(s)}{\log(\log(s))})$ steps.*

Proof. If we want to compute the parity of an s -bit sequence, we can place the s bits as the first row of \mathbf{A} , and set \mathbf{B} to be the all-ones matrix. The least significant bit of the top-left element of the product \mathbf{AB} gives the parity. Since \mathcal{A} only uses the scalar and vector units, it forms an unbounded fan-in Boolean circuit, and therefore Equation (3) gives the result. \square

While the MMU is evidently stronger than the VCU for certain problems, we can show that it is not strong enough by itself to perform arbitrary calculations. That is, even if the VCU implements a “weaker” class of circuits, it still provides crucial capabilities to the model. One example is the following.

Lemma 3.4. *Let s be the MMV-RAM model parameter, and let m, n be two positive integers such that $m = ns$. There exists a vector operation which can be efficiently implemented in the VCU, i.e., with an $AC[0]$ circuit of size m and depth $O(1)$, but it requires $\Omega(n)$ calls to the MMU.*

Proof. One such operation that “troubles” the MMU is a simple block-reordering of a large vector. Assume that we have a vector of size $ms = ns^2$, which is partitioned in ns blocks of size s , and the blocks are grouped in consecutive groups of s blocks each. The goal is to reverse the order of the blocks within each group.

Assume that we only have an MMU available. The rows of a matrix can only be permuted with multiplications from the left. From the definition of the MMU, we can reverse the order of at most s blocks (a single group) at a time with a single matrix multiplication. This means that we need $\Omega(n)$ total calls to the MMU. On the other hand, this reordering can be easily implemented with an $AC[0]$ circuit. \square

3.3 Circuit analysis of the vector unit

In MMV-RAM, the VCU can execute a fixed set of operations that belong to AC[0], in particular, uniform families of unbounded fan-in circuits with constant depth and polynomial size in the input vector length, n . In Table 3.3, we summarize all the vector instructions that are used in Algorithm 4.1. All operations involve one or two vectors of size n with single-bit elements or B -bit integers. Instructions 6-9 are parametrized by s , the (fixed) model parameter. The instructions can be implemented with uniform AC[0] circuits for every input size n as follows.

- The standard operations AND/OR/NOT, can be implemented with size n , depth one, and constant fan-in/-out.
- MASK takes as input a vector \mathbf{x} with integer elements, and a “mask” boolean vector \mathbf{y} , and copies the input element $\mathbf{x}(i)$ to the output position $\mathbf{z}(i)$ if $\mathbf{y}(i) = 1$, otherwise $\mathbf{z}(i)$ is set to zero. It can be achieved by performing a bit-wise AND of each B -bit element $\mathbf{x}(i)$ with $\mathbf{y}(i)$, in depth one, size nB , and constant fan-in/-out.
- ISZERO takes as input a vector with integer elements, and returns a boolean vector \mathbf{z} , such that $\mathbf{z}(i) = 1$ if the corresponding element $\mathbf{x}(i)$ is equal to zero, otherwise $\mathbf{z}(i) = 0$. This can be achieved with a vector of size $O(nB)$, where we simply need to check that all the bits of each element $\mathbf{x}(i)$ are equal to zero, i.e., by negating each bit and using a \vee gate with fan-in $O(B)$ and fan-out one.
- Element-wise ADD/SUB can also be achieved with AC[0] circuits, with $O(nB^2)$ and $O(B)$ fan-in boolean gates. See e.g. [57, Chapter 1] or [20, Chapter 8] for further details and for more advanced circuits and techniques. We note that, in the main algorithm, we only use subtractions $a - b$ for the special case where $a \geq b$.
- FILLS is parametrized by s . It copies the first element of each s -segment of the input vector \mathbf{x} , namely, $\mathbf{x}(is)$, for $i = 0, \dots, \lceil \frac{n}{s} \rceil$, to the corresponding entire segment in the output vector, i.e., $\mathbf{z}(is : (i+1)s)$. The circuit has size $O(nB)$, constant fan-in, and $O(s)$ fan-out.
- SCATTERS/GATHERS are also parametrized by s . As the name suggests, GATHERS copies the last element of the i -th s -segment of \mathbf{x} , to $\mathbf{z}(i-1)$. Accordingly, SCATTERS copies the $(i-1)$ -th element of \mathbf{x} to the last position of the i -th s -segment of \mathbf{z} . The corresponding circuits have size $O(sB)$, since they only copy one element per segment to a single position in the output, and the fan-in/-out of the gates are all constant.
- Finally, the instruction REVSPEC is a uniform circuit that corrects the misspeculated (unsegmented) scans in Algorithm 4.1. This circuit is described in detail in Section 4, specifically, in Lemma 4.1.

4 Segmented scan in MMV-RAM

This section presents a parallel segmented scan in the MMV-RAM model, Algorithm 4.1. The algorithm follows a block-recursive approach described next, with the key feature of exclusively employing vector operations and matrix multiplications.

4.1 A block recursive approach to segmented scan

Here, we outline a block-recursive approach to computing segmented scans, which is the basis of Algorithm 4.1. The core idea of computing segmented scans (recursively) via a contraction argument is well known in the literature; see [5] and [49, Algorithms 3 and 4] for fan-in of size two. Notably, for the unsegmented scan problem, [64] extended the contraction approach to blocks (or fan-in) of size s , generalizing the classic Brent–Kung algorithm [11]. In the following, we briefly describe a similar generalization for the segmented case.

Given an input vector \mathbf{x} and a boolean vector \mathbf{f} both of size n , the block recursive approach initially partitions \mathbf{x} and \mathbf{f} in consecutive blocks of size s . Then the following steps are executed:

1. On each s -block of (\mathbf{x}, \mathbf{f}) , compute (in parallel) the “local” segmented scan and store the result in place on \mathbf{x} .
2. Collect the values $(\mathbf{x}(s-1), \mathbf{x}(2s-1), \dots)$ into a vector \mathbf{x}_s of size $\lceil \frac{n}{s} \rceil$ (pad with zero if necessary).

3. Generate a vector \mathbf{f}_s of size $\lceil \frac{n}{s} \rceil$ by applying the logical OR operator to the elements of each s -block of \mathbf{f} .
4. Recursively compute the segmented scan of $(\mathbf{x}_s, \mathbf{f}_s)$ of size $\lceil \frac{n}{s} \rceil$, and store the result in \mathbf{z}_s .
5. On each s -block, update \mathbf{x} using \mathbf{z}_s by applying the associative binary operation between the last element of the previous block (skip the first block) and each element of the first segment of the current block.

4.2 Putting everything together

Algorithm 4.1 *speculatively* computes the “local” unsegmented scans of each block of size s . Then, the speculated scan will be updated through a REVSPEC vector instruction, which corrects the misspeculated values to complete the local segmented scans.

Algorithm 4.1 Segmented scan in the MMV-RAM model

```

1: procedure SEGSCAN( $\mathbf{x}, \mathbf{f}; s$ )                                     ▶  $s \geq 2$  is the fixed MMV-RAM parameter
2:    $\mathbf{z} \leftarrow \text{BLOCKSEGSCAN}(\mathbf{x}, \mathbf{f}; s)$ 
3:   return RECURSE( $\mathbf{z}, \mathbf{f}; s$ )
4: procedure RECURSE( $\mathbf{z}, \mathbf{f}; s$ )
5:   if  $\text{len}(\mathbf{z}) \leq s$  then
6:     return  $\mathbf{z}$ 
7:    $\bar{\mathbf{f}} \leftarrow \text{MATMUL}(\mathbf{f}, \mathbf{U}_s)$ 
8:    $\bar{\mathbf{f}}_s \leftarrow \text{GATHERS}(\bar{\mathbf{f}}; s)$ 
9:    $\mathbf{f}_s \leftarrow \text{NOT}(\text{ISZERO}(\bar{\mathbf{f}}_s))$                                      ▶ View flags in  $\{0, 1\}$ 
10:   $\mathbf{z}_s \leftarrow \text{GATHERS}(\mathbf{z}; s)$ 
11:   $\mathbf{z}_s \leftarrow \text{BLOCKSEGSCAN}(\mathbf{z}_s, \mathbf{f}_s; s)$ 
12:   $\mathbf{z}_s \leftarrow \text{RECURSE}(\mathbf{z}_s, \mathbf{f}_s; s)$ 
13:   $\mathbf{z} \leftarrow \text{SCATTERS}(\mathbf{z}_s; s)$ 
14:  UPDATEFIRSTSEGMENT( $\mathbf{z}(s-1:), \mathbf{f}(s-1:); s$ )
15:  return  $\mathbf{z}$ 
16: procedure BLOCKSEGSCAN( $\mathbf{x}, \mathbf{f}; s$ )
17:   $\bar{\mathbf{x}} \leftarrow \text{MATMUL}(\mathbf{x}, \mathbf{U}_s)$                                      ▶ Speculative  $s$ -block scan
18:   $\bar{\mathbf{f}} \leftarrow \text{MATMUL}(\mathbf{f}, \mathbf{U}_s)$ 
19:  return REVSPEC( $\bar{\mathbf{x}}, \bar{\mathbf{f}}; s$ )                                     ▶ Revert speculation to form segmented scan
20: procedure UPDATEFIRSTSEGMENT( $\mathbf{z}, \mathbf{f}; s$ )
21:   $\bar{\mathbf{f}} \leftarrow \text{MATMUL}(\mathbf{f}, \mathbf{U}_s)$ 
22:   $\bar{\mathbf{f}}_{start} \leftarrow \text{FILLS}(\bar{\mathbf{f}}; s)$                                      ▶  $\bar{\mathbf{f}}_{start}(is : (i+1)s) = \bar{\mathbf{f}}(is)$ 
23:   $\mathbf{m} \leftarrow \text{ISZERO}(\text{SUB}(\bar{\mathbf{f}}, \bar{\mathbf{f}}_{start}))$                                ▶  $\mathbf{m}(i) = 1$  if  $\bar{\mathbf{f}}(i)$  is equal to the first element of its segment
24:   $\mathbf{m} \leftarrow \text{AND}(\mathbf{m}, \neg \mathbf{f})$                                        ▶ No update on first element of each segment
25:   $\mathbf{w} \leftarrow \text{FILLS}(\mathbf{z}; s)$                                        ▶  $\mathbf{w}(is : (i+1)s) = \mathbf{z}(is)$  (unfiltered correction vector)
26:   $\mathbf{w} \leftarrow \text{MASK}(\mathbf{w}, \mathbf{m})$                                        ▶ Filtered (masked) correction vector
27:   $\mathbf{z} \leftarrow \text{ADD}(\mathbf{z}, \mathbf{w})$ 

```

In particular, at each recursive step, the algorithm computes the “local” segmented scan of each s -block of the input \mathbf{x} in two phases (**BLOCKSEGSCAN** in Algorithm 4.1). In the first phase, we compute the *unsegmented* scans of each block by speculative matrix multiplications using \mathbf{U}_s as the right matrix operand, see Line 17 of Algorithm 4.1. In the second phase, the algorithm reverts any misspeculated segment using vector operations (REVSPEC in Algorithm 4.1). Given an unsegmented scan of any s -block, Lemma 4.1 describes an AC[0] circuit for REVSPEC, which reverts the misspeculated scans. We highlight that such a circuit is only achievable because we have already pre-computed the unsegmented scans of \mathbf{x} and \mathbf{f} .

Lemma 4.1. *Let \mathbf{x} and \mathbf{f} be a value and a boolean vector, each of size s . Assume that we have black-box access to a full scan of \mathbf{x} and \mathbf{f} , i.e., $\widehat{\mathbf{x}}^\top = \mathbf{x}^\top \mathbf{U}_s$ and $\widehat{\mathbf{f}}^\top = \mathbf{f}^\top \mathbf{U}_s$, and assume that the elements of $\widehat{\mathbf{x}}$ and $\widehat{\mathbf{f}}$ fit in B -bit integers. Let \mathbf{z}^* be the segmented scan of \mathbf{x} w.r.t. \mathbf{f} . There exists an AC[0] circuit of size $O(s^2B + B^2)$ which, given $\widehat{\mathbf{x}}$ and $\widehat{\mathbf{f}}$, computes \mathbf{z}^* .*

Proof. The proof is detailed in Appendix A.2. □

To use Lemma 4.1 in Algorithm 4.1, recall that the speculation prepares the entire vectors $\bar{\mathbf{x}} \leftarrow \text{MATMUL}(\mathbf{x}, \mathbf{U}_s)$ and $\bar{\mathbf{f}} \leftarrow \text{MATMUL}(\mathbf{f}, \mathbf{U}_s)$, which contain $O(n/s)$ blocks of size s . By concatenating $\lceil n/s \rceil$ copies of the circuit of Lemma 4.1, we can build a uniform family of circuits that implements the desired vector instruction REVSPEC. The total circuit size is $O(\frac{n}{s}(s^2B + B^2)) = O(n(sB + B^2/s))$, and the depth remains constant after concatenation.

In the last phase of Algorithm 4.1, following the recursive call, the VCU are invoked to scalar-broadcast-vector-add the previous block's last entry (scalar) to the current block's first segment (**UPDATEFIRSTSEGMENT** in Algorithm 4.1).

Indeed, **UPDATEFIRSTSEGMENT** corrects the values of the first segment of each s -block following the recursive call. Specifically, the last entry of a block must be broadcast added to the first segment of the corresponding next block. Again, the selective broadcast add is implemented with an unsegmented scan on \mathbf{f}_s and (masked) vector operations.

Figure 4.1 depicts an example of an execution of Algorithm 4.1 for an input of size 16 and block size $s = 4$. In this example, matrix multiplication computes the unsegmented scans, and the misspeculated entries are coloured red. The reversion of the speculation is followed before the recursions take place. In the final step, vector-masked operations are employed to propagate the last entry of each block to the first segment of the next block.

Remark 4.2. *The circuit of Lemma 4.1 is ideal for our theoretical analysis, but it is rather complicated compared to the rest of the vector instructions in Table 3.3. In a realistic setting, it would need to be implemented as a dedicated circuit inside the VCU, which can be prohibitive in terms of area. In Appendix A.3 we describe an alternative, Algorithm A.2, which simulates the REVSPEC instruction using only a few standard vector instructions, which are typically implemented in existing architectures.*

Why is speculation used for segmented scan? At this point, we explain why speculation is employed and why it seems essential to compute segmented scans in the MMV-RAM model. The first argument is due to the linear algebraic structure of matrix multiplication, which does not allow us to handle arbitrary segment ranges with a single matrix multiplication operation. To see this, assume that we want to compute the segmented scans of s consecutive blocks of length s of some vector \mathbf{x} of length s^2 . Let \mathbf{A} be a matrix with s rows and columns containing \mathbf{x} in row-wise order. Since the rows of \mathbf{A} can have completely different segment ranges, each row of \mathbf{A} must be multiplied with a *different* square matrix of size s from the right to compute its local segmented scan. In the general case, it is impossible to encode all segmented scans of all rows with a single (right) matrix multiplication. Speculation overcomes this algebraic restriction by (speculatively) computing all s unsegmented scans of each s -block via $\mathbf{A}\mathbf{U}_s$, which are later corrected using the VCU. The second reason why speculation is crucial, is that the segmented scans **cannot** be computed efficiently without the speculative scans, as already reported in Theorem 4.4.

4.3 Analysis

Here, we analyze Algorithm 4.1 in terms of the number of steps (depth), the number of vector operations, and the number of matrix multiplications. First, we note that if the input flag vector \mathbf{f} is equal to zero, we recover the unsegmented scan algorithm (prefix sum) of [64], which is a generalization of the Brent-Kung algorithm [11]. In this case, we can completely avoid calling REVSPEC. In Theorem 4.3 we report the complexity of the algorithm of [64] in the MMV-RAM model, which was originally analyzed in the TCU model. The work-depth bounds match the ones of [64] with respect to n and s .

Theorem 4.3 (Scan). *Given a vector \mathbf{x} with integer entries bounded by $x_i \leq M$, for some M , we can compute a vector \mathbf{z} that contains the scan of \mathbf{x} in the MMV-RAM model using the algorithm of [64] (listed in Algorithm 4.2). The algorithm requires:*

- $O(\log_s(n))$ steps,

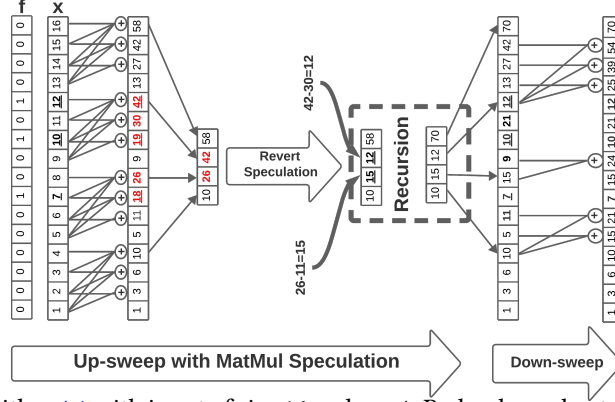


Figure 4.1: Example of Algorithm 4.1 with input of size 16 and $s = 4$. Red-coloured entries are computed speculatively and must be reverted before recursion. Underscored entries mark a segment start.

Algorithm 4.2 Scan in the MMV-RAM model (simplified version of [64, Algorithm 2])

1: **procedure** SCAN($x; s$) ▷ $s \geq 2$ is the MMV-RAM parameter
2: $n \leftarrow \text{len}(x)$
3: $z \leftarrow \text{MATMUL}(x, U_s)$
4: **if** $n \leq s$ **then**
5: **return** z
6: $x_s \leftarrow \text{GATHERS}(z; s)$
7: $z_s \leftarrow \text{SCAN}(x_s; s)$
8: $z \leftarrow \text{SCATTERS}(z_s; s)$
9: $z(s-1:n) \leftarrow \text{MATMUL}(z(s-1:n), B_s)$ ▷ B_s is the identity with all-ones in the first row
10: **return** z

- $O\left(\mathcal{M}\left(\frac{n}{s}\right) + nB^2\right)$ work,
- $B \in O(\log(n) + \log(M))$ bits-per-element to avoid overflow.

Any algorithm that uses only the VCU and executes $n^{O(1)}$ work requires $\Omega\left(\frac{\log(n)}{\log(\log(n))}\right)$ steps.

Proof. At each recursion step, the array size is reduced by a factor of s . Therefore, the recursion depth is $O(\log_s(n))$. Regarding the cost of matrix multiplications, at each iteration $t = 1, \dots, \lfloor \log_s(n) \rfloor$, the algorithm performs two MATMUL operations between two matrices with sizes of size $O(n/s^t) \times s$ and $s \times s$, respectively. The cost of these operations is $\mathcal{M}(n/2^t)$ each. There are also three vector instructions per iteration: one SCATTERS, GATHERS. They both have work (circuit size) $O(sB)$. We therefore have the following recursive formula for the work at iteration t :

$$W(t) = W(t+1) + 2\mathcal{M}\left(\frac{n}{s^t}\right) + O(sB) = \sum_{t=1}^{\lfloor \log_s(n) \rfloor} \mathcal{M}\left(\frac{n}{s^t}\right) + O(sB \log_s(n)) \in O\left(\mathcal{M}\left(\frac{n}{s}\right) + sB \log_s(n)\right).$$

The total number of bits used to store numbers during the execution of the algorithm is bounded as follows. In iteration $t = 1, \dots, \log_s(n)$, we have two MATMUL operations. These are the only operations that can increase the magnitude of the elements. Let $M(1) = M$, and denote by $M(t)$ the magnitude of the largest element at step t . Since the right-hand-side matrices have only zeros and ones, then every matrix multiplication can increase the magnitude of the input elements at most by a factor of s . We then have

$$M(t) \leq s^2 M(t-1) \in O(s^{2 \log_s(n)} M) = O(n^2 M),$$

which means that $O(\log(n) + \log(M))$ bits are sufficient to avoid overflow. □

We can now prove our main Theorem 4.4.

Theorem 4.4 (Segmented Scan). *Given a value vector \mathbf{x} with elements bounded in magnitude by $|\mathbf{x}(i)| \leq M$, and a boolean vector \mathbf{f} , both of size n , Algorithm 4.1 computes the segmented scan \mathbf{z} of \mathbf{x} over \mathbf{f} in the MMV-RAM model. It requires:*

- $O(\log_s(n))$ steps,
- $O\left(\mathcal{M}\left(\frac{n}{s}\right) + nB\left(s + \frac{B}{s}\right)\right)$ work,
- $B \in O(\log(n) + \log(M))$ bits-per-element to avoid overflow.

Any algorithm that uses only the VCU and executes work that scales polynomially in n requires $\Omega\left(\frac{\log(n)}{\log(\log(n))}\right)$ steps.

Proof of Theorem 4.4. The analysis is almost the same as in Theorem 4.3. The recursion depth is again $O(\log_s(n))$. Regarding the total work, in each recursive step $t = 1, \dots, \lfloor \log_s(n) \rfloor$ we need to execute four MATMUL operations of length $O(n/s^t)$, and few vector instructions. The most expensive VCU instruction is REVSPEC, which, from Table 3.3, requires $O\left(\frac{n}{s^t}(sB + B^2/s)\right)$. Thus, the total work becomes

$$W(t) = W(t+1) + 4\mathcal{M}\left(\frac{n}{s^t}\right) + O\left(\frac{n}{s^{t-1}}(sB + B^2/s)\right) = O\left(\mathcal{M}\left(\frac{n}{s}\right) + n(sB + B^2/s)\right).$$

Once again, in the “down sweep” phase, the two operations that can increase the magnitude of elements are two consecutive MATMUL operations. REVSPEC can only decrease the magnitude. In the “up-sweep” phase, we have an ADD instruction that can increase the magnitude of elements by a factor of two, or, equivalently, by a single bit. Therefore, the number of required bits to avoid overflow is upper bounded by the bits required in Theorem 4.3. \square

5 Practical algorithms for segmented operations

Having established complexity bounds, we build on the idea of speculative computation from the previous sections and switch gears to design practical algorithms for segmented operations. To be fully clear, by “practical” we mean algorithms that are simple to describe as compositions of basic primitives and lend themselves to efficient implementations. To that end, the design objective is to avoid the use of deep recursions, the potentially expensive memory layout operations of Algorithm 4.1, as well as complex, dedicated vector instructions, such as REVSPEC. Leveraging MMV-RAM primitives, we devise algorithms for segmented sum (Algorithm 5.1) and scan (Algorithm 5.2). The theoretical complexity of the composed algorithms almost matches the one of the main Algorithm 4.1, i.e., it achieves the same number of steps, but requires some additional work.

5.1 Segmented sum (SCD)

First, we present an algorithm for the segmented sum Problem 2.2, called² SCD, specialized for matrix multiplication accelerators (Algorithm 5.1). The speculative approach in Section 4 allowed us to rethink the segmented sum computation as a composition of three parallel primitives: scan, compress, and vector differentiation. In the first step of SCD, the unsegmented scan of the input \mathbf{x} is computed speculatively! In the second step, \mathbf{f} is slightly modified to \mathbf{f}^- so that the end positions of all segments are marked by the ones in \mathbf{f}^- . Indeed, \mathbf{f}^- is obtained by \mathbf{f} by shifting the vector to the left and appending 1 at the end. Then, the scanned values of \mathbf{x} corresponding to the end position of all segments are collected through a parallel compaction/compress operation using \mathbf{f}^- . It is easy to verify that the segmented sum can be obtained by applying vector differentiation $\mathbf{z}_{\text{diff}}(i) = \mathbf{z}(i) - \mathbf{z}(i-1)$ (assume $\mathbf{z}(-1) = 0$) on the output vector of compress.

Now, we argue that all three steps of SCD could benefit from a MMU, i.e., SCD is amenable to an efficient implementation in the MMV-RAM model. The scan can be implemented using matrix multiplications as shown in [17, 64]. Similarly, parallel compress is typically implemented by first scanning the input flag vector to calculate

²SCD stands for Scan, Compress, and Differentiation.

the output indices. Finally, the DIFF step of SCD could also employ the MMU as described in Appendix A.4 but with very low utilization of the MMU.

To the best of our knowledge, the derivation of segmented sum as a composition of scan, compress, and vector differentiation, has not been explicitly discussed in the literature, but similar ideas exist. One relevant example is the “fast segmented sum”, Algorithm 6 of [37], which we call FSS from now on. Similarly to SCD, FSS performs an unsegmented scan on \mathbf{x} . FSS requires an additional copy of the input data vector to a temporary vector. Next, using the additional temporary vector, FSS computes the segmented sums using a gather in a parallel for-loop. In contrast, and crucially, SCD does not require an additional temporary vector and could take advantage of the MMU for the index calculations of the parallel compaction/compress operation. We highlight that Algorithm 5.1 can be implemented in the same number of steps as Algorithm 4.1 with some appropriate modifications, albeit, by executing additional work (up to a factor of n). This is due to the COMPRESS operation, which internally needs to gather elements from arbitrary positions, and, therefore, such a “GATHER” circuit needs to have all-to-all connections to do this in constant depth uniformly.

Algorithm 5.1 Segmented Sum \cong
DIFF \circ COMPRESS \circ SCAN

```

1: procedure SCD( $\mathbf{x}$ ,  $\mathbf{f}$ )
2:    $\widehat{\mathbf{x}} \leftarrow \text{SCAN}(\mathbf{x})$             $\triangleright$  Speculative scan.
3:    $\mathbf{f}^- \leftarrow \mathbf{f}(1 :)$  appended with 1
4:    $\mathbf{z} \leftarrow \text{COMPRESS}(\widehat{\mathbf{x}}, \mathbf{f}^-)$ 
5:    $\mathbf{z}_{\text{diff}} \leftarrow \text{DIFF}(\mathbf{z})$     $\triangleright$  Vector Differentiation.
6:   return  $\mathbf{z}_{\text{diff}}$ 

```

Algorithm 5.2 Segmented Scan \cong
REVERT \circ COMPRESS \circ (SCAN, SCAN)

```

1: procedure SSCR( $\mathbf{x}$ ,  $\mathbf{f}$ )
2:    $(\widehat{\mathbf{x}}, \widehat{\mathbf{f}}) \leftarrow (\text{SCAN}(\mathbf{x}), \text{SCAN}(\mathbf{f}))$ 
3:    $\mathbf{f}^- \leftarrow \mathbf{f}(1 :)$  appended with 1
4:    $\mathbf{w} \leftarrow \text{COMPRESS}(\widehat{\mathbf{x}}, \mathbf{f}^-)$ 
5:   parfor  $\text{idx}$  in  $\text{len}(\mathbf{w})$  do            $\triangleright$  REVERT.
6:      $\mathbf{z} \leftarrow \widehat{\mathbf{x}} - (\widehat{\mathbf{f}} == \text{idx} + 1) \cdot \mathbf{w}(\text{idx})$ 
7:   return  $\mathbf{z}$ 

```

5.2 Segmented scan (SSCR)

The segmented scan algorithm, dubbed³ SSCR (Algorithm 5.2), shares a similar approach to the SCD algorithm. Similarly to SCD, SSCR performs a speculative scan of \mathbf{x} and then a parallel compress to collect the last entries of each segment. In addition, SSCR requires a scan of the boolean flag vector along with a parallel correction operation that could be performed in the VCU (Lines 5-6 of Algorithm 5.2). We call the vector-only correction operator *REVERT* (not to be confused with the REVSPEC AC[0] circuit of Table 3.3). The worst-case work/step complexity of SSCR in the MMV-RAM model is the same as Algorithm 5.1, i.e., both algorithms can be implemented in $\mathcal{O}(\log_s(n))$ steps, similar to Algorithm 4.1.

6 Applications of segmented operations

In this section, we show how to perform higher-level operations in the MMV-RAM model, by using Algorithm 4.1 as a subroutine. In both cases, we reduce the number of steps (depth) from $\mathcal{O}(\log(n))$ to $\mathcal{O}(\log_s(n))$ while performing the same amount of work (up to polylogarithmic factors) with the corresponding vector-only algorithms (AC[0] circuits).

6.1 Element-wise integer vector multiplications using segmented sums

The first application of our segmented scan algorithm in the MMV-RAM model is the element-wise multiplication between two vectors with integer elements. We first recall that two integers with B bits each cannot be multiplied with an AC[0] circuit (since parity reduces to integer multiplication [57]). From the lower bound of Theorem 3, this means that any boolean circuit for integer multiplication $B^{\mathcal{O}(1)}$ size will have $\Omega\left(\frac{\log(B)}{\log \log(B)}\right)$ depth. Using Algorithm 4.1 as the building block, we can exploit the MMU to achieve a circuit of smaller depth and polynomial size.

³SSCR stands for Scan, Scan, Compress and Revert.

Lemma 6.1. *Let a and b be two integers with magnitudes $|a|, |b| \leq M \leq 2^B$. In the MMV-RAM model, we can compute the product ab with:*

- $O(\log_s(B))$ steps,
- $O\left(\mathcal{M}\left(\frac{B}{s}\right) + sB^2\right)$ work,
- $B \in O(\log(M))$ bits-per-element to avoid overflow.

Proof. Let $m = \lceil \log(M) \rceil$. Following the “school method” (e.g. [57, Chapter 1]), we know that we can write:

$$ab = \sum_{i=0}^{m-1} c_i, \quad \text{where } c_i := \begin{cases} \underbrace{0 \dots 0}_{2m-1} a_{m-1} \dots a_1 a_0 \underbrace{0 \dots 0}_i, & \text{if } b_i = 0, \\ \underbrace{0 \dots 0}_{2m-1}, & \text{otherwise.} \end{cases}$$

Now, each c_i can be prepared with a circuit of size $O(m)$ in constant depth, which gives a total size of $O(m^2)$ for all c_i 's, and each c_i consists of $2m - 1$ bits. We can put the c_i 's in a vector \mathbf{c} of length B , and use Theorem 4.3 to compute a full scan of \mathbf{c} in $O(\log_s(m))$ steps and $O\left(\mathcal{M}\left(\frac{m}{s}\right) + sm^2\right)$ work. The last element of the scanned vector contains ab . In terms of avoiding overflow, Theorem 4.4 indicates that $B \in O(\log(m) + m) = O(\log(M))$ bits are sufficient. \square

Corollary 6.2. *Let \mathbf{x} and \mathbf{y} be two vectors with integer elements bounded by $|\mathbf{x}(i)|, |\mathbf{y}(i)| \leq M$. We can compute their element-wise product with an algorithm $\mathbf{z} \leftarrow \text{MULT}(\mathbf{x}, \mathbf{y})$ in the MMV-RAM model, with*

- $O(\log_s(B))$ steps,
- $O\left(\mathcal{M}\left(\frac{nB}{s}\right) + nsB^2\right)$ work.
- $B \in O(\log(n) + \log(M))$ bits to avoid overflow.

Proof. For each element $\mathbf{z}(i) = \mathbf{x}(i)\mathbf{y}(i)$, we can compute a SCAN as in Lemma 6.1. This can be done collectively for all i with a segmented scan operation (Algorithm 4.1), where each segment corresponds to one $\mathbf{z}(i)$. \square

6.2 Matrix multiplication

In this section, we provide a work/depth analysis of the standard, inner product-based matrix multiplication algorithm in the MMV-RAM model. The segmented scan Algorithm 4.1 and the integer vector multiplication algorithm of Corollary 6.2 form the main building blocks. The main idea here is to exploit the MMU to perform the final reductions, after the scalar (or block) multiplications. To see the potential impact, consider first a matrix multiplication algorithm that is split in two-phases: (i) scalar products and (ii) reductions to form the final matrix product. Even if we obtain the scalar multiplications (i) “for free”, we still need to compute the reductions (ii). If we use only the VCU for this task, we need to execute $\Omega(\log(n)/\log \log(n))$ steps. The same holds if, instead of scalar products, we use the MMU in phase (i) to compute matrix products of small $s \times s$ blocks. That is, we still need to reduce these small products in the second phase, in order to form the final matrix product. The reductions require $\Omega(\log(\frac{n}{s})/\log \log(\frac{n}{s}))$ steps with the VCU. Notably, in the following Theorem 6.3 we obtain an algorithm with only $O(\log_s(nB))$ step complexity and nearly $O(n^3)$ work.

Theorem 6.3. *Let \mathbf{A} and \mathbf{B} be two $n \times n$ matrices with non-negative integer entries that are bounded in magnitude by M . In the MMV-RAM model, we can compute the product $\mathbf{C} = \mathbf{AB}$ with*

- $O(\log_s(nB))$ steps,
- $O\left(\mathcal{M}\left(\frac{n^3B}{s}\right) + n^3sB^2\right)$ work
- $O(\log(n) + \log(M))$ bits per output element to avoid overflow.

Any matrix multiplication algorithm that requires to perform reductions between blocks of size $O(s) \times O(s)$ with the VCU necessarily requires $\Omega\left(\frac{\log(n/s)}{\log(\log(n/s))}\right)$ steps.

Proof. There exists an AC[0] circuit with size $O(n^3B)$ which prepares two vectors \mathbf{a} and \mathbf{b} , with size n^3 each. In particular, \mathbf{a} contains n concatenated copies of a flattened version of the matrix \mathbf{A} , while \mathbf{b} contains n copies of the first column of \mathbf{B} , followed by n copies of the second column, n copies of the third column, and so on. This way, the vector multiplication $\mathbf{c} \leftarrow \text{MULT}(\mathbf{a}, \mathbf{b})$, will contain all the integer scalar products needed by the standard dot product-based matrix multiplication algorithm. Using Corollary 6.2 the total work is $O\left(\mathcal{M}\left(\frac{n^3B}{s}\right) + n^3sB^2\right)$ and the number of steps $O(\log_s(B))$. We then do an additional segmented scan using Algorithm 4.1, which, from Theorem 4.4, requires $O\left(\mathcal{M}\left(\frac{n^3}{s}\right) + nB\left(s + \frac{B}{s}\right)\right)$ work and $O(\log_s(n))$ steps. In terms of bits to avoid overflow, the first segmented scan requires $O(\log(M))$ bits from Lemma 6.1, while the second requires $O(\log(n) + \log(M))$, from Theorem 4.4. \square

7 Experiments

This section evaluates the proposed MMV-RAM algorithms. Since the MMV-RAM model is general and suitable for any architecture combining multiple MMU and VCU, we target Ascend 910B accelerators as a use case. Moreover, as we want to prove the effectiveness of algorithms in the MMV-RAM model with respect to their vector-only version, we tailor each algorithm for the same architecture, the Ascend accelerator, which suits the MMV-RAM model.

7.1 Evaluation setup

In this section, we evaluate the performance of our implemented algorithms. We remark that such implementations generally suit architectures fitting the MMV-RAM model, as GPUs with both matrix and vector cores, AMD NPUs, considering part of compute tiles used to build a matrix core (for example, through a systolic array) and remaining used as vector cores [27], and Ascend AI Cores 910B, combining matrix multiplication (cube) units and 40 VCU. All proposed algorithms were implemented in C++17 using the AscendC programming framework. We used the Ascend CANN toolkit 8.0.RC2.alpha003 with Ascend firmware and drivers versions 1.0 and 23.0.0, respectively. All evaluations are performed on the Ascend 910B accelerator of Huawei [36]. All experiments were performed using an AMD EPYC CPU processor running on Ubuntu 22.04. We used the PyTorch Ascend adaptor⁴ with version v2.4.0 to report all our PyTorch-related measurements. To wrap our custom AscendC segmented operators in PyTorch, we used the pybind11 and PyTorch C++ extension functionality. Time measurements are collected using the PyTorch profiler. Each time measurement is averaged, through arithmetic mean, over 100 repetitions.

Ascend 910B Accelerator. The architecture of Ascend accelerators, namely the DaVinci architecture, combines a MMU, called a Cube unit, with VCU and scalar processors in multiple cores [36, 35]. Additionally, each core is linked with Memory Transfer Engines (MTE) that transfer data between global / local buffers, and a hierarchy of intermediate scratchpad memories to store intermediate tiled data.

An AI cube core is primarily responsible for matrix multiplication, whereas AI vector cores offer SIMD capabilities. Lastly, the scalar vector can be used to perform scalar/index computations required by the data-parallel cores.

The programming model is asynchronous and pipeline-based, as multiple AI core executions can be pipelined while data flows from one unit to the other, optimizing performance. Computational kernels could be written in AscendC, a programming language built on top of C++ allowing for fine-grained control over the hardware components of Ascend. As the accelerator specifically targets AI workloads, in which we can usually apply quantization to handle data sizes, it mainly offers support for int8, float16, and float32, making the accelerator suitable for both training and inference steps; see [35] for further details.

⁴The Ascend PyTorch adaptor is open-sourced at <https://gitee.com/ascend/pytorch>.

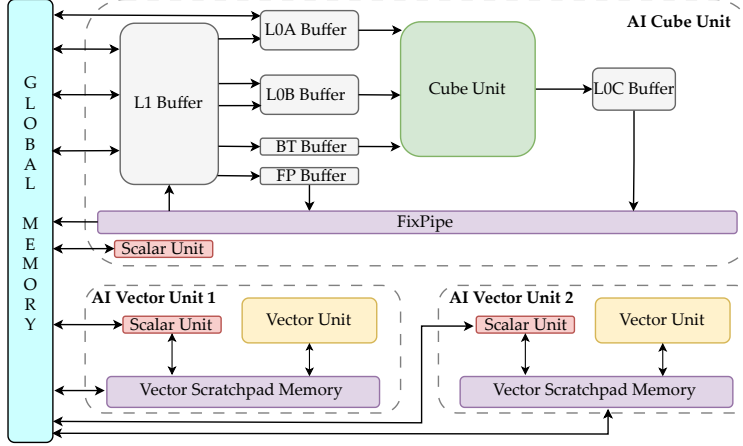


Figure 7.1: Architecture of an AI core of the Ascend 910B AI Accelerator. Each AI core consists of one Cube (matrix multiplication) unit and two vector cores. The architecture mounts 20 AI Cores.

Implementation of Ascend operators. Here, we provide implementation details regarding the parallel primitive operators. For unsegmented scans, we use the best available scan implementation for Ascend, which also makes heavy use of the MMU. This scan implementation, SCAN, supports both as inputs half/float16 and integers with bit-width 8 (int8) with output data types float32 and int32, respectively. For vector differentiation (DIFF), we use the implementation provided by Ascend’s software stack. For compress (COMPRESS), we use the best available implementation that also makes heavy use of the MMU. COMPRESS is implemented by first scanning f , which has data type int8, followed by a gather vector operation. Finally, we implemented the REVERT kernel as a vector-only operator, as it is not straightforward how to use the MMU for this task.

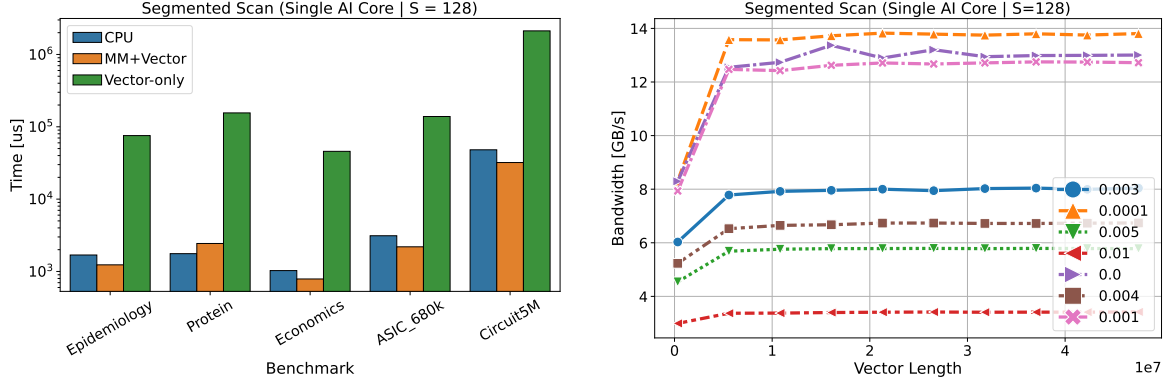
7.2 Experimental results

In this section, we first evaluate the performance of a single AI core Ascend 910B implementation of Algorithm 4.1. Next, in section 7.2.2, we evaluate a multi-core implementation of SCD and a multi-core implementation of SSCR on the Ascend 910B accelerator.

7.2.1 Segmented scan using a single AI core

Here, we evaluate the performance benefits that result from using the cube unit (MMU) of the Ascend accelerator for segmented scans. We implemented a single Ascend AI core following Algorithm 4.1. Recall that an Ascend AI core consists of one Cube core and two vector cores. As a first step, the implementation uses the Cube core to perform s consecutive scans each of length s . We set $s = 128$ to maximize the L0A/L0B scratchpad memories of the cube unit. In the second step, these speculative block scans are transferred to the VCU to revert the speculative scans as in Algorithm A.1 (see Appendix A.3). Notice that we serialize the parallel for-loop in Line 10 of Algorithm A.1. Also, we split each matrix tile of length s^2 (a matrix tile has size $s \times s$) into two halves and assign one half matrix tile to one vector core. Each vector core is responsible for producing the segmented scan output on one half, while on the other half tile, the same vector core only keeps track of the correct (accumulation) value needed for the next matrix tile iteration. Here, we avoid the expensive vector-core synchronization using recomputation. As a baseline segmented scan method, we implement a *vector-only* algorithm that performs the speculative scan within the VCU, using the cumsum AscendC API, and then performs the speculation. We call the baseline method “Vector-only”. We also report the performance of a C++ (compiler optimization flag O3) CPU implementation using a vanilla for-loop segmented scan for reference.

Figure 7.2 provides an experimental evaluation of the above single Ascend AI core implementation of Algorithm 4.1. In particular, Figure 7.2 (a) depicts the performance comparison, showing that the MM+V version is more



(a) Segmented scan (single AI core) versus vector-only 910B cores and single-thread CPU C++ (-O3).

(b) Segmented scan over uniformly random segments. Single core memcopy achieves $\approx 60\text{GB/s}$.

Figure 7.2: Single Ascend AI 910B core segmented scan implementation based on Algorithm 4.1.

efficient than the vector-only baseline. We also measure the performance of a single-thread C++ CPU implementation for normalization purposes. Interestingly enough, the MM+V approach has performance comparable to that of a single-thread CPU vanilla implementation. For the analysis, we chose five different matrices from various scenarios, from epidemiology to economics. Such matrices have already been chosen from previous related works [37], and their dimensions span from $36K \times 36K$ up to $5M \times 5M$ (further information in Table A.1).

The above observation also agrees with the theoretical analysis of the MMV-RAM model, where, in Section 3, we argued that there is a clear theoretical advantage of having a MMU.

Figure 7.2 (b) depicts the performance of the single-core segmented scan algorithm on various segment density levels drawn uniformly at random. Segment density is the ratio of the number of ones in f over the length of f . We used densities in the range of 0.1% up to 1% to assess the potential performance degradation for dense scenarios. As can be observed, we achieve nearly the same performance as in the unsegmented scan case for low density ($\approx 0.1\%$). For density equal to 0.01, the algorithm performs better than the unsegmented case due to the particular two-vector core implementation⁵ that we used. Finally, we observe that the performance is two times lower for density in the range 0.3 – 0.5%.

7.2.2 Practical and multi-core segmented operations

This section evaluates a preliminary implementation of the segmented sum (SCD) and segmented scan (SSCR) algorithms presented in Section 5. Our goal here is two-fold.

The first objective is to provide a preliminary analysis of the relative performance of the parallel primitives used in these algorithms. Such a performance analysis of their components could identify opportunities for performance improvements in a highly optimized implementation for SCD and SSCR in the future. Providing a high-performance implementation that, for example, fuses these parallel primitives is a non-trivial task, and we leave it as future work.

Second, we provide performance evaluation of matrix multiplication-based implementations, whenever possible, of the parallel primitives. For their analysis, we measure the bandwidth, comparing such primitives with a baseline memcopy/copy operator, which provides the device bandwidth limits. Such a “roof-line” type of experimental analysis allows us to argue about the peak performance of each parallel primitive [60]. Of course, such an analysis does not take into consideration performance optimizations due to operator fusion and the benefits of the existence of an L2 cache between global memory and the Ascend AI cores. However, breakdown analysis is valuable for identifying key bottlenecks.

Figure 7.3 depicts an execution time breakdown of the parallel primitives used in the SCD (left figure) and SSCR (right figure) algorithms. In both figures, the matrix multiplication tile size, s , is set to 128 and the density of segments

⁵Our two-vector core method is not the best possible for the unsegmented scan case, and it could be potentially improved by using binary search when computing the accumulation value on the half matrix tile.

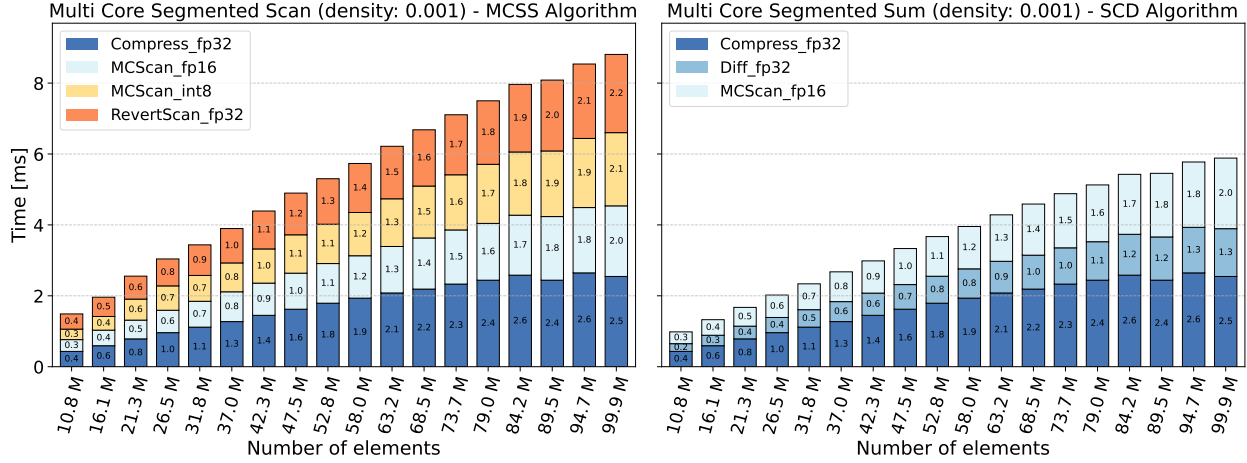


Figure 7.3: Execution time breakdowns for SCD (Algorithm 5.1, left) and SSCR (Algorithm 5.2, right).

is 0.1%. Both figures show that COMPRESS takes a large fraction of the execution time, i.e., around 50% and around 33% for SCD and SSCR, respectively. The DIFF operator implementation on Ascend has almost identical performance to the data copy operator, see also Figure 7.4. Both COMPRESS and SCAN have similar performance in the left figure. In the SSCR figure, we observe that the REVERT operation takes a considerable fraction of the elapsed time.

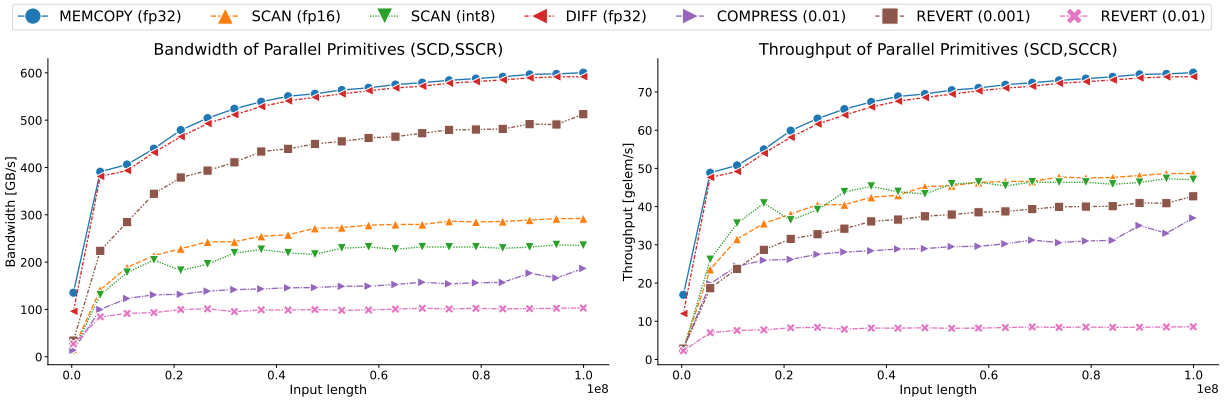


Figure 7.4: Bandwidth/throughput of parallel primitives (Section 5) versus memory copy operator. The peak theoretical bandwidth is 800GB/s.

To further analyze the operators, on the left of Figure 7.4, we depict the performance of the parallel primitives (SCAN, COMPRESS, DIFF and REVERT) used in the segmented operations in Section 5. The left subfigure shows the bandwidth performance of the operators compared to a memory copy operator for increasing input lengths. Since all operators are memory-bound, the plot demonstrates that the performance of each operator is close to the peak memory bandwidth offered by the device. The bandwidth performance of REVERT for segment density 0.001 is surprisingly higher than the performance of our best scan operator.

On the right of Figure 7.4, we depict the performance of the parallel primitives (scan, compress, diff, revert) used in the segmented operations. We plot the performance of the primitive operators with respect to the number of input elements (of the input vector x) per second processed. We set the segment density equal to 0.001. The y -axis depicts billions (Giga) elements per second (Gelem/s). The performance (Gelem/s) of the scan operators (both fp16 and int8) is better compared to the compress and revert operators, which is expected since both revert and compress read additional int32 inputs to encode the segments. The performance of REVERT with segment density equal to 1%

has the lowest performance around 10 Gelem/s.

8 Extensions of MMV-RAM

In this section, we briefly discuss possible variants and extensions of the MMV-RAM model.

8.1 Different circuit classes for the VCU

The VCU of MMV-RAM consists of AC[0] circuits. Other circuit complexity classes might be worth investigating, and what is their effect in the analysis of algorithms. As an example, recall that our main algorithms for segmented operations rely on gates with fan-in and fan-out of $\mathcal{O}(\text{poly}(s, B))$ size, i.e., independent of input size. Some hardware implementations, however, might only support constant fan-in gates. As such, NC[0] can be investigated as an alternative for the VCU. Other classes can also be considered depending on the applications. Some other examples from [57] include semi-bounded fan-in circuits (SAC), AC “with counters” (ACC), or AC[0] circuits extended with additional modulo gates. These classes lie between NC[0] and NC[1] in the so-called NC-hierarchy (cf. [57, Chapter 4]). In all cases, the complexity of VCU instructions (size-depth) and the balance with the MMU should be carefully calibrated.

8.2 Extending the right-hand-side of the MMU

Given two input matrices A and B with sizes $n \times s$ and $s \times s$, the MMU of MMV-RAM computes $C = AB$ in a single step. There is a clear asymmetry between A and B . If we partition A into blocks of size $s \times s$, i.e., $A = (A_1^\top \ A_2^\top \ A_2^\top \ \dots)^\top$, then each block A_i is multiplied with the same matrix B from the right. It is reasonable to ask whether we can build a more powerful (and/or more “symmetric”) model by allowing each block A_i to be multiplied with a different matrix B_i from the right. For example, assuming a total of k blocks of size $s \times s$, the MMU now computes

$$\begin{pmatrix} A_1 B_1 \\ \vdots \\ A_k B_k \end{pmatrix} \leftarrow \begin{pmatrix} A_1 \\ \vdots \\ A_k \end{pmatrix} \odot \begin{pmatrix} B_1 \\ \vdots \\ B_k \end{pmatrix}, \quad \text{instead of} \quad \begin{pmatrix} A_1 B \\ \vdots \\ A_k B \end{pmatrix} \leftarrow \begin{pmatrix} A_1 \\ \vdots \\ A_k \end{pmatrix} B.$$

In this modification, the MMU acts as a “block-vector unit”, executing small matrix multiplications between blocks. Such an extension seems particularly interesting, for example, for large matrix multiplications. Indeed, assuming any matrix multiplication algorithm that can be written as a bilinear circuit, the scalar product gates can be replaced with block-wise multiplications of size $s \times s$. However, our efforts so far did not reveal any significant advantages of this extension over the proposed MMV-RAM definition of Section 3. The main reason is the following. The (depth) hardness of matrix multiplication arises from the parity problem: in any bilinear circuit for matrix multiplication, all scalar multiplications can be executed in constant depth, but the reductions of these scalar products to obtain the bilinear forms necessarily require a logarithmic number of steps (if the circuit size remains polynomial). Our Theorem 6.3 indicates that we can perform (large) matrix multiplications in $\mathcal{O}(\log_s(n))$ steps in MMV-RAM. On the other hand, in the extended model, the number of steps can potentially be reduced to $\mathcal{O}(\log_s(n/s))$, which barely saves a constant number of steps. Based on these observations, the possible benefits of this seemingly natural model extension are yet to be clarified, and left as future research.

9 Conclusion & future work

We proposed a machine model for matrix multiplication / AI accelerators, called MMV-RAM, which extends the Vector-RAM model with matrix multiplication processing units. A detailed analysis was provided, rigorously balancing the computational power between the vector and matrix multiplication units.

In the MMV-RAM model, we designed and analyzed a segmented scan algorithm that uses both VCUs and MMU and runs in $\mathcal{O}(\log_s(n))$ steps. The key idea of the algorithm is to perform speculative block scans using the MMU, which are later corrected using the VCU. Beyond the worst-case complexity analysis, we also presented algorithms

for segmented operations that could be translated into efficient implementations on real systems. In addition, we provided a preliminary experimental evaluation of our MMV-RAM algorithms using the Ascend AI 910B accelerator.

Several different directions can be envisioned for future research. As mentioned in Section 8, different extensions and variants of the MMV-RAM model can be further investigated. Such an analysis can yield better insights not only for algorithmic innovations but also for novel architecture designs for future accelerators, e.g., by identifying critical primitive operations as well as algorithmic bottlenecks. On the practical and algorithmic side, further studies can be conducted for other fundamental applications, such as sparse matrix computations, aiming at both practical and theoretical improvements.

References

- [1] Advanced Micro Devices, Inc.: AMD CDNA™ 4 Architecture. White Paper 2258402, Advanced Micro Devices, Inc. (2025), <https://www.amd.com/content/dam/amd/en/documents/instinct-tech-docs/white-papers/amd-cdna-4-architecture-whitepaper.pdf>
- [2] Alman, J., Duan, R., Williams, V.V., Xu, Y., Xu, Z., Zhou, R.: More asymmetry yields faster matrix multiplication. In: Proceedings of the ACM-SIAM Symposium on Discrete Algorithms (SODA). pp. 2005–2039 (2025). <https://doi.org/10.1137/1.9781611978322.63>
- [3] Alman, J., Yu, H.: Improving the leading constant of matrix multiplication. In: Proceedings of the ACM-SIAM Symposium on Discrete Algorithms (SODA). pp. 1933–1971. SIAM (2025)
- [4] Ballard, G., Demmel, J., Holtz, O., Lipshitz, B., Schwartz, O.: Communication-optimal parallel algorithm for Strassen’s matrix multiplication. In: Proceedings of Symposium on Parallelism in Algorithms and Architectures (SPAA). pp. 193–204 (2012)
- [5] Blelloch, G.E.: Scans as primitive parallel operations. *IEEE Transactions on Computers* **38**(11), 1526–1538 (1989). <https://doi.org/10.1109/12.42122>
- [6] Blelloch, G.E.: Prefix sums and their applications. In: *Synthesis of parallel algorithms*, pp. 35–60. Morgan Kaufmann (1990)
- [7] Blelloch, G.E.: *Vector models for data-parallel computing*. MIT Press, Cambridge, MA, USA (1990)
- [8] Blelloch, G.E.: Programming parallel algorithms. *Communications of the ACM* **39**(3), 85–97 (Mar 1996). <https://doi.org/10.1145/227234.227246>
- [9] Blelloch, G.E., Heroux, M.A., Zagha, M.: Segmented operations for sparse matrix computation on vector multiprocessors. Tech. rep., Carnegie Mellon University, USA (1993)
- [10] Borodin, A.: On relating time and space to size and depth. *SIAM Journal on Computing* **6**(4), 733–744 (1977). <https://doi.org/10.1137/0206054>
- [11] Brent, R.P., Kung, H.T.: The chip complexity of binary arithmetic. In: *Proceedings of the Symposium on Theory of Computing (STOC)*. p. 190–200. ACM (1980). <https://doi.org/10.1145/800141.804666>
- [12] Chatterjee, S., Blelloch, G.E., Zagha, M.: Scan primitives for vector computers. In: *Proceedings of the 1990 ACM/IEEE conference on Supercomputing*. pp. 666–675 (1990)
- [13] Chen, B., Dao, T., Liang, K., Yang, J., Song, Z., Rudra, A., Re, C.: Pixelated butterfly: Simple and efficient sparse training for neural network models. In: *International Conference on Learning Representations (ICLR)* (2022)
- [14] Chowdhury, R., Silvestri, F., Vella, F.: A computational model for tensor core units. In: *Proceedings of Symposium on Parallelism in Algorithms and Architectures (SPAA)*. p. 519–521. ACM (2020). <https://doi.org/10.1145/3350755.3400252>

- [15] Chowdhury, R., Silvestri, F., Vella, F.: Algorithm design for tensor units. In: International Conference on Parallel and Distributed Computing (Euro-Par). p. 353–367. Springer-Verlag (2021)
- [16] Culler, D., Karp, R., Patterson, D., Sahay, A., Schauser, K.E., Santos, E., Subramonian, R., Von Eicken, T.: LogP: Towards a realistic model of parallel computation. In: Proceedings of Symposium on Parallelism in Algorithms and Architectures (SPAA). pp. 1–12 (1993)
- [17] Dakkak, A., Li, C., Xiong, J., Gelado, I., Hwu, W.m.: Accelerating reduction and scan using tensor core units. In: Proceedings of ACM International Conference on Supercomputing (ICS). p. 46–57. ICS '19, ACM (2019). <https://doi.org/10.1145/3330345.3331057>
- [18] Dave, S., Baghdadi, R., Nowatzki, T., Avancha, S., Shrivastava, A., Li, B.: Hardware acceleration of sparse and irregular tensor computations of ML models: A survey and insights. Proceedings of the IEEE **109**(10), 1706–1752 (2021). <https://doi.org/10.1109/JPROC.2021.3098483>
- [19] Demmel, J., Dumitriu, I., Holtz, O., Kleinberg, R.: Fast matrix multiplication is stable. Numerische Mathematik **106**(2), 199–224 (2007)
- [20] Dhall, S.K.: Parallel computing using the prefix problem. Oxford University Press, Inc., USA (1994)
- [21] Furst, M., Saxe, J.B., Sipser, M.: Parity, circuits, and the polynomial-time hierarchy. Mathematical systems theory **17**(1), 13–27 (1984)
- [22] Håstad, J.: Almost optimal lower bounds for small depth circuits. In: Proceedings of the Symposium on Theory of Computing (STOC). pp. 6–20. ACM (1986)
- [23] Harvey, D., Van Der Hoeven, J.: On the complexity of integer matrix multiplication. Journal of Symbolic Computation **89**, 1–8 (2018)
- [24] He, X., Pal, S., Amarnath, A., Feng, S., Park, D.H., Rovinski, A., Ye, H., Chen, Y., Dreslinski, R., Mudge, T.: Sparse-TPU: Adapting systolic arrays for sparse matrices. In: Proceedings of International Conference on High-Performance Computing, Networking, Storage and Analysis (SC). pp. 1–12 (2020)
- [25] Hoefler, T., Alistarh, D., Ben-Nun, T., Dryden, N., Peste, A.: Sparsity in deep learning: pruning and growth for efficient inference and training in neural networks. J. Mach. Learn. Res. **22**(1) (Jan 2021)
- [26] Hong, J.W., Kung, H.T.: I/O complexity: The red-blue pebble game. In: Proceedings of the Symposium on Theory of Computing (STOC). pp. 326–333 (1981)
- [27] Hunhoff, E., Melber, J., Denolf, K., Bisca, A., Bayliss, S., Neuendorffer, S., Fifield, J., Lo, J., Vasireddy, P., James-Roxby, P., Keller, E.: Efficiency, Expressivity, and Extensibility in a Close-to-Metal NPU Programming Interface . In: 2025 IEEE 33rd Annual International Symposium on Field-Programmable Custom Computing Machines (FCCM). pp. 85–94. IEEE Computer Society, Los Alamitos, CA, USA (May 2025). <https://doi.org/10.1109/FCCM62733.2025.00043>
- [28] JáJá, J.: An introduction to parallel algorithms. Addison Wesley Longman Publishing Co., Inc., USA (1992)
- [29] Jouppi, N.P., et al.: In-datacenter performance analysis of a tensor processing unit. In: Proceedings of International Symposium on Computer Architecture (ISCA). p. 1–12. ACM (2017). <https://doi.org/10.1145/3079856.3080246>
- [30] Jouppi, N.P., et al.: Ten lessons from three generations shaped google’s TPUv4i: Industrial product. In: Proceedings of International Symposium on Computer Architecture (ISCA). pp. 1–14 (2021). <https://doi.org/10.1109/ISCA52012.2021.00010>
- [31] Kaplan, J., McCandlish, S., Henighan, T., Brown, T.B., Chess, B., Child, R., Gray, S., Radford, A., Wu, J., Amodei, D.: Scaling laws for neural language models (2020), <https://arxiv.org/abs/2001.08361>

- [32] Krizhevsky, A., Sutskever, I., Hinton, G.E.: Imagenet classification with deep convolutional neural networks. In: *Advances in Neural Information Processing Systems (NIPS)*. p. 1097–1105 (2012)
- [33] Kung, H., McDanel, B., Zhang, S.Q.: Packing sparse convolutional neural networks for efficient systolic array implementations: Column combining under joint optimization. In: *Proceedings of International Conference on Architectural Support for Programming Languages and Operating Systems (ASPLOS)*. pp. 821–834 (2019)
- [34] Ladner, R.E., Fischer, M.J.: Parallel prefix computation. *Journal of ACM* **27**(4), 831–838 (Oct 1980). <https://doi.org/10.1145/322217.322232>
- [35] Liao, H., Tu, J., Xia, J., Liu, H., Zhou, X., Yuan, H., Hu, Y.: Ascend: a scalable and unified architecture for ubiquitous deep neural network computing: industry track paper. In: *Proceedings of International Symposium on High-Performance Computer Architecture (HPCA)*. pp. 789–801. IEEE (2021). <https://doi.org/10.1109/HPCA51647.2021.00071>
- [36] Liao, H., Tu, J., Xia, J., Zhou, X.: DaVinci: A scalable architecture for neural network computing. In: *Hot Chips Symposium on High-Performance Chips (HCS)*. pp. 1–44 (2019). <https://doi.org/10.1109/HOTCHIPS.2019.8875654>
- [37] Liu, W., Vinter, B.: CSR5: An efficient storage format for cross-platform sparse matrix-vector multiplication. In: *Proceedings of ACM International Conference on Supercomputing (ICS)*. p. 339–350. ICS '15, ACM (2015). <https://doi.org/10.1145/2751205.2751209>
- [38] Markidis, S., Chien, S.W.D., Laure, E., Peng, I.B., Vetter, J.S.: Nvidia tensor core programmability, performance & precision. *arXiv preprint arXiv:1803.04014* (2018)
- [39] McColl, W.F.: General purpose parallel computing. *Lectures on parallel computation* **4**, 337–391 (1993)
- [40] McColl, W.F.: Scalable computing. *Computer Science Today: Recent Trends and Developments* pp. 46–61 (2005)
- [41] McColl, W.F., Tiskin, A.: Memory-efficient matrix multiplication in the BSP model. *Algorithmica* **24**, 287–297 (1999)
- [42] Mishra, A., Latorre, J.A., Pool, J., Stosic, D., Stosic, D., Venkatesh, G., Yu, C., Micikevicius, P.: Accelerating sparse deep neural networks (2021), <https://arxiv.org/abs/2104.08378>
- [43] NVIDIA Corporation: NVIDIA A100 Tensor Core GPU Architecture (2020), <https://www.nvidia.com/content/dam/en-zz/Solutions/Data-Center/nvidia-ampere-architecture-whitepaper.pdf>
- [44] Okanovic, P., Kwasniewski, G., Labini, P.S., Besta, M., Vella, F., Hoefler, T.: High performance unstructured spmm computation using tensor cores. In: *Proceedings of International Conference on High-Performance Computing, Networking, Storage and Analysis (SC)*. SC '24, IEEE Press (2024). <https://doi.org/10.1109/SC41406.2024.00060>
- [45] Parekh, O., Phillips, C.A., James, C.D., Aimone, J.B.: Constant-depth and subcubic-size threshold circuits for matrix multiplication. In: *Proceedings of Symposium on Parallelism in Algorithms and Architectures (SPAA)*. pp. 67–76 (2018)
- [46] Pratt, V.R., Rabin, M.O., Stockmeyer, L.J.: A characterization of the power of vector machines. In: *Proceedings of the Symposium on Theory of Computing (STOC)*. pp. 122–134 (1974)
- [47] Raz, R.: On the complexity of matrix product. In: *Proceedings of the Symposium on Theory of Computing (STOC)*. pp. 144–151 (2002)
- [48] Raz, R., Shpilka, A.: Lower bounds for matrix product, in bounded depth circuits with arbitrary gates. In: *Proceedings of the Symposium on Theory of Computing (STOC)*. pp. 409–418 (2001)

- [49] Sengupta, S., Harris, M., Zhang, Y., Owens, J.D.: Scan primitives for GPU computing. In: Proceedings of the 22nd ACM SIGGRAPH/EUROGRAPHICS Symposium on Graphics Hardware. p. 97–106. GH '07, Eurographics Association, Goslar, DEU (2007)
- [50] Shiloach, Y., Vishkin, U.: Finding the maximum, merging and sorting in a parallel computation model. In: Conpar 81: Conference on Analysing Problem Classes and Programming for Parallel Computing Nürnberg, June 10–12, 1981 Proceedings. pp. 314–327. Springer (1981)
- [51] Solomonik, E., Demmel, J.: Communication-optimal parallel 2.5D matrix multiplication and LU factorization algorithms. In: European Conference on Parallel Processing. pp. 90–109. Springer (2011)
- [52] Strassen, V.: Gaussian elimination is not optimal. *Numerische mathematik* **13**(4), 354–356 (1969)
- [53] Talpes, E., Sarma, D.D., Venkataramanan, G., Bannon, P., McGee, B., Floering, B., Jalote, A., Hsiong, C., Arora, S., Gorti, A., Sachdev, G.S.: Compute solution for tesla’s full self-driving computer. *IEEE Micro* **40**(2), 25–35 (2020). <https://doi.org/10.1109/MM.2020.2975764>
- [54] Tiskin, A.: The bulk-synchronous parallel random access machine. *Theoretical Computer Science* **196**(1-2), 109–130 (1998)
- [55] Valiant, L.G.: A bridging model for parallel computation. *Communications of the ACM* **33**(8), 103–111 (1990)
- [56] Vaswani, A., Shazeer, N., Parmar, N., Uszkoreit, J., Jones, L., Gomez, A.N., Kaiser, L., Polosukhin, I.: Attention is all you need. In: Advances in Neural Information Processing Systems (NIPS). p. 6000–6010. NIPS'17, Curran Associates Inc. (2017)
- [57] Vollmer, H.: Introduction to circuit complexity: a uniform approach. Springer Science & Business Media (1999)
- [58] Wang, Y., Zhang, C., Xie, Z., Guo, C., Liu, Y., Leng, J.: Dual-side sparse tensor core. In: Proceedings of International Symposium on Computer Architecture (ISCA). p. 1083–1095. ISCA '21, IEEE Press (2021). <https://doi.org/10.1109/ISCA52012.2021.00088>
- [59] Wegener, I.: The complexity of Boolean functions. John Wiley & Sons, Inc. (1987)
- [60] Williams, S., Waterman, A., Patterson, D.: Roofline: an insightful visual performance model for multicore architectures. *Commun. ACM* **52**(4), 65–76 (Apr 2009). <https://doi.org/10.1145/1498765.1498785>
- [61] Williams, V.V., Xu, Y., Xu, Z., Zhou, R.: New bounds for matrix multiplication: from alpha to omega. In: Proceedings of the ACM-SIAM Symposium on Discrete Algorithms (SODA). pp. 3792–3835. SIAM (2024)
- [62] Yao, A.C.C.: Separating the polynomial-time hierarchy by oracles. In: Proceedings of the Symposium on Foundations of Computer Science (FOCS). pp. 1–10. IEEE (1985)
- [63] Zachariadis, O., Satpute, N., Gómez-Luna, J., Olivares, J.: Accelerating sparse matrix–matrix multiplication with GPU tensor cores. *Computers & Electrical Engineering* **88**, 106848 (2020). <https://doi.org/10.1016/j.compeleceng.2020.106848>
- [64] Zouzias, A., McColl, W.F.: A parallel scan algorithm in the tensor core unit model. In: International Conference on Parallel and Distributed Computing (Euro-Par). Lecture Notes in Computer Science, vol. 14100, pp. 489–502. Springer (2023). https://doi.org/10.1007/978-3-031-39698-4_33

A Appendix

A.1 Matrix multiplication circuits

In this appendix, we provide the corresponding background and existing results for matrix multiplication circuits, which were outlined in Table 3.2.

We first recall two arithmetic circuit sub-classes from [48, 47]. *Bounded-coefficient* arithmetic circuits impose the restriction that all weights and inputs of product gates have magnitude at most one. *Bilinear* arithmetic circuits consist of three subcircuits Σ_1 , Π , and Σ_2 . The subcircuit Σ_1 receives as inputs the elements of the two matrices and contains only $\{+\}$ gates (of unbounded fan-in). The second subcircuit, Π , consists of only one level of $\{\times\}$ gates with fan-in two. The inputs of these $\{\times\}$ gates are the outputs of Σ_1 . Finally, Σ_2 contains only $\{+\}$ gates, which receive as inputs the outputs of Π . The outputs of Σ_2 are the elements of the matrix product.

Arithmetic circuits. The arithmetic complexity of multiplying two $s \times s$ matrices (in terms of scalar additions and multiplications) is $\mathcal{O}(s^{\omega+\eta})$, for any $\eta > 0$, where the currently best known upper bound for the exponent is $\omega < 2.371339$ [2]. Depth-size trade-offs for general arithmetic circuits were thoroughly studied by Raz and Shpilka [48]. The authors proved that any matrix multiplication arithmetic circuit with size S and depth d can be transformed into an equivalent bilinear circuit of size $\mathcal{O}(S)$ and depth $\mathcal{O}(d)$, and that any bilinear circuit whose longest path from the product gates to the outputs has length $d \leq 1$ necessarily has size $\Omega(s^3)$. The standard dot-product based matrix multiplication algorithm achieves this size and depth. For arbitrary $d \geq 2$, the authors proved a $\Omega(\frac{\lambda_d(s^2)}{d^2} s^2)$ size lower bound, where $\lambda_d(s^2)$ is a family of slow-growing functions, in particular, $\lambda_2(x) = \log(x)$, $\lambda_3(x) = \log(\log(x))$ (see [48] for more details). Raz [47] proved an $\Omega(s^2 \log(s))$ lower bound for the size of any bounded-coefficient arithmetic circuit for matrix multiplication, including depth-size tradeoffs.

Boolean circuits. For the multiplication of integer matrices using (unbounded fan-in) boolean circuits, depth lower bounds can be directly obtained from the parity problem [21, 62, 22]. To see this, note that a sequence $X \in \{0, 1\}^n$ can be copied to the first row of a $\{0, 1\}^{n \times n}$ matrix A . Then one can compute the product AB where B is the all-ones matrix. The least significant bit of the top-left element of the result gives the parity of X . This means that any constant-depth matrix multiplication boolean circuit necessarily has exponential size, which can be achieved, for example, by “brute-forcing” the corresponding DNF.

Threshold circuits. Threshold circuits were thoroughly analyzed in [45]. Focusing on Strassen’s algorithm ([52]) as a baseline, the authors proved several size-depth trade-offs. One of the main contributions that we import here is a TC[0] circuit with size $\mathcal{O}(s^{3-\delta})$ for some $\delta \in (0, 1)$ to multiply two $s \times s$ matrices with $\mathcal{O}(\log(s))$ -bit integer elements. It is also outlined how to extend the analysis for other fast matrix multiplication algorithms besides Strassen’s. Size lower bounds can be obtained from [48] for this case as well. The aforementioned $\Omega(\frac{\lambda_d(s^2)}{d^2} s^2)$ size lower bound of [48] also holds for boolean circuits with arbitrary gates (including threshold circuits) for matrix multiplication over GF[2]. The latter directly reduces to integer matrix multiplication, which gives the lower bound.

Finally, to simulate rectangular matrix multiplications of size $m \times s$ and $s \times s$, for arbitrary m , there are many different options. The simplest is to assume m/s copies of a square matrix multiplication circuit of size $s \times s$, such as the standard inner-product algorithm or the TC[0] circuits of [45]. Alternatively, one can consider circuits dedicated to rectangular matrix multiplications (recall that two matrices of size $s \times s^\alpha$ and $s^\alpha \times s$ can be multiplied in $\mathcal{O}(s^2)$ arithmetic operations for all $\alpha \lesssim 0.32$ [2, 61]). Other specialized circuits can be used, for example, if the matrices have very large entries [23].

To conclude this section, we can mention the following works regarding other aspects of matrix multiplication algorithms. [41] provides a detailed analysis in the BSP model. The numerical stability of fast matrix multiplication algorithms in the floating point model was studied in [19]. Communication and I/O complexity have been analyzed in [26, 4, 51]. Finally, we refer to the recent work of [3], which heavily reduces the leading constants of fast matrix multiplication algorithms.

A.2 Proof of Lemma 4.1

In this appendix we provide the proof of Lemma 4.1, which we restate for readability.

Lemma A.1 (Restatement of Lemma 4.1). *Let \mathbf{x} and \mathbf{f} be a value and a boolean vector, each of size s . Assume that we have black-box access to a full scan of \mathbf{x} and \mathbf{f} , i.e., $\widehat{\mathbf{x}}^\top = \mathbf{x}^\top \mathbf{U}_s$ and $\widehat{\mathbf{f}}^\top = \mathbf{f}^\top \mathbf{U}_s$, and assume that the elements of $\widehat{\mathbf{x}}$ and $\widehat{\mathbf{f}}$ fit in B -bit integers. Let \mathbf{z}^* be the segmented scan of \mathbf{x} w.r.t. \mathbf{f} . There exists an AC[0] circuit of size $O(s^2B + B^2)$ which, given $\widehat{\mathbf{x}}$ and $\widehat{\mathbf{f}}$, computes \mathbf{z}^* .*

Proof. We are given as input the two scanned vectors $\widehat{\mathbf{x}}$ and $\widehat{\mathbf{f}}$, both of size s . Recall the elements of $\widehat{\mathbf{f}}$ indicate the index of the segment where each element of \mathbf{x} belongs. From each segment, we need to subtract the last element of the previous segment. In the final vector \mathbf{z}^* , the element $\mathbf{z}^*(j)$, $j \in [s]$, is equal to the corresponding element $\widehat{\mathbf{x}}(j)$ minus the last element of the previous segment. More specifically, for all $j = 1, \dots, s$, we must subtract from $\widehat{\mathbf{x}}(j)$ the element $\widehat{\mathbf{x}}(i)$, for some $i < j$, if and only if both the following conditions hold simultaneously:

1. $\widehat{\mathbf{f}}(i) \neq \widehat{\mathbf{f}}(i+1)$: true, if segment ends at index i ,
2. $\widehat{\mathbf{f}}(j) = \widehat{\mathbf{f}}(i+1)$: true, if index j is in next segment.

To perform this subtraction efficiently, we will prepare an “update vector” \mathbf{u} , which contains B -bit integer elements, and each element $\mathbf{u}(j)$ will be subtracted from $\widehat{\mathbf{x}}(j)$. To that end, we first construct a binary “filter matrix” \mathbf{Q} , whose elements encode the above conditions 1. and 2., in particular:

$$\mathbf{Q}(i, j) \leftarrow \begin{cases} \left(\widehat{\mathbf{f}}(i) \neq \widehat{\mathbf{f}}(i+1) \right) \wedge \left(\widehat{\mathbf{f}}(j) = \widehat{\mathbf{f}}(i+1) \right), & \text{if } j > i, \\ 0, & \text{else.} \end{cases}$$

The elements of the matrix \mathbf{Q} can be prepared by a circuit of constant depth and size $O(s^2B)$.

Given \mathbf{Q} , we can write the elements of \mathbf{u} as

$$\mathbf{u}(j) \leftarrow \bigvee_{i=1}^{j-1} \widehat{\mathbf{x}}(i) \wedge \mathbf{Q}(i, j),$$

where in this case we slightly abuse the \bigvee and \wedge notation, since $\widehat{\mathbf{x}}(i)$ is a B -bit integer, and therefore $\widehat{\mathbf{x}}(i) \wedge \mathbf{Q}(i, j)$ indicates that the “ \wedge ” gate operates on all the bits of $\widehat{\mathbf{x}}$ one-by-one. The size of this circuit is $O(s^2B)$, and the depth is again constant.

Finally, having prepared \mathbf{u} , we can set $\mathbf{z}^* \leftarrow \widehat{\mathbf{x}} - \mathbf{u}$. The final subtraction can be done in constant depth and size $O(B^2)$. Putting everything together, the final circuit for \mathbf{z}^* has constant depth and size $O(s^2B + B^2)$. \square

A.3 Reverting speculative scans using (masked) vector operations

Here, we demonstrate that the REVSPEC vector operation can be simulated using multiple masked vector operations. We present two such algorithms.

First, Algorithm A.1 is simple and provides insight about the vector computations required. Its main drawback is that it performs reductions of $O(s)$ numbers for each segment, hence requiring $O(\log(s))$ steps and $O(ns)$ work. To further reduce the work overhead of the speculation, we present Algorithm A.2, which has $O(n \log(s))$ work and $\log(s) + O(1)$ steps. The key difference of the two algorithms is that the latter uses a Kogge–Stone prefix masked reduction to avoid the work overhead (recomputation) compared to Algorithm A.1.

Algorithm A.1 Revert Speculative Prefix Sums

```
1: procedure REVERTSPECSIMPLE( $\mathbf{z}$ ,  $\mathbf{x}$ ,  $\mathbf{f}$ ,  $s$ ) ▷ Works in-place on  $\mathbf{z}$ 
2:    $\bar{\mathbf{f}} \leftarrow \text{MATMUL}(\mathbf{f}, \mathbf{U}_s)$ 
3:   parfor each  $s$ -block ( $\mathbf{z}_s, \mathbf{x}_s, \bar{\mathbf{f}}_s$ ) do
4:      $\mu \leftarrow \bar{\mathbf{f}}_s(s - 1)$ 
5:     if  $\mu == 0$  or ( $\mu == 1$  and  $\bar{\mathbf{f}}_s(0) == 1$ ) then
6:       return ▷ Speculation is correct.
7:     if  $\mu == s$  then
8:        $\mathbf{z}_s \leftarrow \mathbf{x}_s$  ▷  $s$  segments, no scan required. Revert.
9:       return
10:    parfor  $\text{idx} = \bar{\mathbf{f}}_s(0) + 1, \dots, \mu$  do
11:       $\text{offset} \leftarrow \text{SUM}(\text{LESSLTHAN}(\bar{\mathbf{f}}_s, \text{idx})) - 1$ 
12:       $\mathbf{z}_s \leftarrow \mathbf{z}_s - (\bar{\mathbf{f}}_s == \text{idx}) \cdot \mathbf{z}_s(\text{offset})$ 
```

A.4 Vector differentiation using matrix multiplications

Here, we demonstrate that it is possible to use matrix multiplication to compute vector differentiation in the last step of Algorithm 5.1. Let \mathbf{A} be a row-wise matrix view with s columns of an arbitrary vector \mathbf{x} (padded accordingly). Let

$$\mathbf{D}_s := \begin{bmatrix} 1 & -1 & 0 & \dots & 0 \\ 0 & 1 & -1 & \dots & 0 \\ 0 & 0 & 1 & \dots & 0 \\ \vdots & 0 & 0 & \ddots & -1 \\ 0 & 0 & \dots & 0 & 1 \end{bmatrix}_{s \times s}. \quad (4)$$

It is easy to verify that the matrix product $\mathbf{A}\mathbf{D}_s$ computes the difference $x_i - x_{i-1}$ on each s -block except the boundary entries between blocks. The remaining entries on the boundary can be computed using the VCU.

A.5 Dataset details

Table A.1 shows the matrix characteristics, including matrix sizes and sparsity statistics of the matrices used in Section 7.

Table A.1: Sparse Suite Matrices.

| Name | Dimensions | nnz | nnz per row | | nnz per row |
|--------------|--------------------|------|-------------|-----|-------------|
| | | | in | avg | max |
| Protein | 36K \times 36K | 4.3M | 2K | 2K | 2K |
| Epidemiology | 526K \times 526K | 2.1M | 18 | 119 | 204 |
| Economics | 207K \times 207K | 1.3M | 1 | 6 | 44 |
| Circuit5M | 5.6M \times 5.6M | 2.1M | 18 | 119 | 204 |
| ASIC_680K | 683K \times 683K | 3.9M | 1 | 6 | 395K |

Algorithm A.2 Revert Speculative Scans with MMV-RAM Vector instructions

```
1: procedure REVERTSPECMMVDRAM( $z, x, f, s$ ) ▷ Works in-place on  $z$ 
2:    $\bar{f} \leftarrow \text{MATMUL}(f, U_s)$ 
3:   parfor each  $s$ -block ( $z_s, x_s, \bar{f}_s$ ) do
4:      $\mu \leftarrow \bar{f}_s(s - 1)$ 
5:     if  $\mu == 0$  or ( $\mu == 1$  and  $\bar{f}_s(0) == 1$ ) then
6:       return ▷ Speculation is correct.
7:     if  $\mu == s$  then
8:        $z_s \leftarrow x_s$  ▷  $s$  segments, return input.
9:       return
10:     $q_s \leftarrow \text{XOR}(\text{SHIFTL}(\bar{f}, 1), f)$ 
11:     $m_s \leftarrow \text{SHIFTR}(q_s, 1)$ 
12:     $w_s \leftarrow \text{SHIFTR}(\text{MASK}(z_s, q_s), 1)$  ▷ Correction vector.
13:    for  $j = 0, \dots, \lceil \log(s) \rceil$  do
14:       $b \leftarrow 2^j$ 
15:       $\bar{m}_s \leftarrow \text{SHIFTR}(m_s, b)$ 
16:       $\bar{w}_s \leftarrow \text{SHIFTR}(w_s, b)$ 
17:       $filter_s \leftarrow \text{LEQ}(\text{ADD}(m_s, \bar{m}_s), 2)$ 
18:       $m_s \leftarrow \text{MASK}(\text{ADD}(m_s, \bar{m}_s), filter_s)$ 
19:       $w_s \leftarrow \text{MASK}(\text{ADD}(w_s, \bar{w}_s), filter_s)$ 
20:     $z_s \leftarrow \text{SUB}(z_s, w_s)$ 
```
